Prototype Testing of Improved Microtunnelling Pipes

by

C. C. Holt
G. W. E. Milligan
H. J. Burd

University of Oxford
Department of Engineering Science
Parks Road
Oxford
OX1 3PJ

EXECUTIVE SUMMARY

The research project described in this report is stage 5 in an ongoing research programme that is currently being undertaken at Oxford University. Projects to data have included laboratory model and material testing, field instrumentation and monitoring of full scale pipe jacks under construction and finite element analysis. This research project is a continuation of stage 4 of the research programme in which finite element analyses and laboratory testing identified possible design improvements to microtunnelling pipes. The purpose of stage 5 was to test these design improvements at prototype scale.

The project consisted of two phases. The first involved the detailed design of the test rig and data acquisition equipment. The test rig was designed to test DN600 microtunnelling pipes to failure at deflection angles of 0.5^{o} and 1.0^{o}. The maximum safe working load capacity of the test rig was 6000 kN. Data acquisition consisted of: (a) load cells to measure jacking forces, (b) Electro-levels to monitor pipe and rig rotation and (c) video records of failure mechanisms.

The second phase of the project involved the design and incorporation of joint modifications to the spigot end of DN600 microtunnelling pipes. ARC Pipes, Stanton Bonna Concrete Ltd. and Hepworth Building Products each supplied twelve pipes. Modifications incorporated to ARC and Stanton Bonna pipes included a 2^{o} or 3^{o} chamfer, local internal joint reinforcement and a combination of joint chamfer and localised internal joint reinforcement. The modifications incorporated into Hepworth pipes included the placement of a single or double prestressed steel band at the spigot joint. Standard production pipes from each manufacturer were tested for comparison Purposes. Pipes were tested at a deflection angle of 0.5^{o} or 1.0^{o}.

For all pipes tested no spalling was observed at the spigot end during the application of load. Pipes with a chamfered joint experienced a reduction in load capacity of between 2.3% and 20.8% compared with a standard production pipe. Reductions in strength were greater for a 3^{o} chamfer than for a 2^{o} chamfer. Although the introduction of localised internal joint reinforcement into pipes incorporating a joint chamfer increased the load capacity, the strength was less than that of a standard production pipe. When internal reinforcement was introduced into a standard production pipe the load capacity increased by between 2.9% and 10.6%. The placement of one external prestressed steel band at the spigot end increased the load capacity by between 12.8% and 19.1%. However, when two external prestressed bands were incorporated the capacity of the pipe decreased by between 9.5% and 12.6% compared with a standard production pipe.

The research led to some interesting findings. Further work, particularly numerical analysis is required so that a better understanding of the failure mechanisms is achieved.

ACKNOWLEDGEMENTS

The research described in this report was funded jointly by the PJA, North West Water, Severn Trent Water, Thames Water and EPSRC.

The authors of this report would like to thank the following for their input into the research programme:

All those at ARC pipes who supplied pipes and helped considerably with the testing programme, especially Will Spur, Mark Flavell, Charlie and the men in the works.

Stanton Bonna Concrete for supplying pipes, and technical assistance from Rob Fifer and Fred Bamford.

Jeff Bridges of Hepworths Building Products for supplying pipes

David Morgan of Tunnelling Accessories for supplying the packing material for testing, usually at very short notice.

John Bunce of Barhale Equipment Ltd. for manufacturing the external prestressed steel bands.

Decon Engineering for manufacturing the test rig.

David Partridge of Landsowne Engineering Services for modifying the test rig

The PJA for their technical assistance.

CONTENTS

1. INTRODUCTION

The UK is engaged in a major programme of updating its infrastructure in water supply and sewerage, driven by European legislation and increased public expectation following the privatisation of the water industry. There is also continuing demand for the provision of new services requiring underground ducting, both in the UK and overseas.

Trenchless technologies are becoming a popular method for installing new pipe lines and ducting. Pipe jacking is a typical trenchless technology and is used for forming small diameter tunnels and pipe lines by progressively jacking a string of pipes through the ground from a thrust pit to a reception pit. Additional pipes are added at the thrust pit as the tunnel advances by manual or mechanical means. For pipes of non-man-entry sizes (less than 1000mm internal diameter) this procedure is described as micro-tunnelling. Excavation of material from the pipes is by mechanical means and is controlled remotely, usually from the ground surface. Larger diameter pipes, typically up to 3000mm internal diameter are also machine excavated, but can also be hand excavated.

Jacking pipes are usually most heavily loaded during installation; once in place they are more than adequate to sustain long-term ground loading etc. Work carried out at Oxford University indicates that the performance of pipes during jacking is largely controlled by the behaviour of the pipe joints. As no pipe line can be perfectly straight, small angular deflections occur at the joints; this gives rise to highly localised stresses at the pipe ends. Analyses and field monitoring have shown that even well-controlled drives, the loaded area is only a small sector of the pipe end. Packing material placed in the pipe joints help to distribute the longitudinal stresses, although, even with the best available materials, high stresses still occur near the outside edge of the pipe. This can lead to local spalling at relatively low working loads and in more severe cases local failure. Spalling of the pipe joint may damage the integrity of the seal, and expose the reinforcement

A recent research project at Oxford University investigated the effects of high localised stresses at the pipe joints caused by adjacent pipe misalignment. Finite element analyses and laboratory testing techniques were used to assess possible pipe design improvements. Results suggested that with minor modifications to the pipe joints jacking loads on typical pipe jacks could be increased by as much as 20%, and more importantly spalling at working loads eliminated.

Because the jacking loads are restricted by the joint capacity, the pipe barrel is relatively lightly stressed. At present the majority of pipes are reinforced (with the exception of some microtunnelling pipes) throughout their length with a longitudinal bars with spirally-wound hoop reinforcement. The previous research suggests that the barrel of the pipe could be less heavily reinforced, and that more localised reinforcement is needed at the joint. This would have the advantage of reducing manufacturing costs. Other potential benefits are clear: fewer failures of pipes during jacking; the possibility of

longer and more economical drives; reduction in non-detectable defects and reduced long-term maintenance or replacement costs.

The purpose of this current research project is to investigate the performance of modified pipes at full-scale. The testing programme compared standard production pipes and pipes with a chamfered joint profile, local joint reinforcement and a combination of reinforcement and a chamfer. The localised joint reinforcement comprised either externally placed prestressed steel bands or internally placed hoop reinforcement.

A new test rig was constructed in order to carry out the tests. The rig was capable of loading to failure DN600 microtunnelling pipes at deflection angles of 0.5^{o} and 1.0^{o}.

This report summarises the design and development of the test rig and the modifications incorporated into the standard production pipes. A summary of all pipe failures is also presented along with a detailed discussion of failure mechanisms. Conclusions are drawn and areas of further work suggested.

2. BACKGROUND TO CURRENT RESEARCH PROJECT

2.1 Significance of pipeline alignment

In any pipe-jacking operation it is important to ensure that angular misalignments between adjacent pipe segments are kept to an absolute minimum. If misalignments do occur then this leads to concentrations of stresses at the pipe joints which can, in extreme cases, lead to failure of the pipe. In an ideal pipe jack, no such deviations would occur. In practice, however, irregularities in ground conditions, excavation methods, etc., may cause the shield at the front of the pipe jack to divert from the intended course. This may be compensated by continual small steering corrections by the steering jacks to maintain the line and level. The pipe line therefore "wriggles" through the ground, and since the pipes are relatively rigid small angular deviations occur at the pipe joints, Figure 2.1. These angular misalignments can generate additional interface friction between pipes and soil, and more significantly reduce the jacking load that can be transmitted safely through the pipe joints.

These small angular deviations were shown theoretically Ripley (1989), and later confirmed in practice by site measurements Norris (1992), to produce highly localised areas of stress between pipe joint faces. This may lead to spalling and joint damage, ultimately causing serious cracking in the pipes. These effects can jeopardise the long-term integrity of the pipe, and in serious cases even prevent completion of the pipe installation.

2.2 Alignments achieved in practice

A deviation of as little as 0.5^{o} between adjacent pipes can produce highly localised stresses at the joint face of the pipe. Norris (1992) monitored pipe jacks at five different instrumented sites with varying soil conditions, cover depths and at various locations within the pipe string. This study included the logging of deflection angles of the joints during jacking by using special instrumentation and from conventional line and level measurements. Typical results from these instrumented sites are given in Figure 2.2. The β angle (also referred to in this report as "deflection angle") in this figure represents the angular misalignment between adjacent pipes. Typically drives were within the specified line and level throughout the jack and typical joint angles ranged between 0.0^{o} and 0.3^{o}, with a maximum deflection angle of up to approximately 0.5^{o}. These drives were well controlled; in poorly controlled drives or where ground conditions are adverse, deflection angles may exceed 1.0^{o}.

Norris (1992) found that alignment control tended to be poorest at the start of a drive. The data also demonstrated that the alignment of the pipeline (in its unloaded state) did not change significantly as the pipeline was extended; thus local curvatures once established remain throughout the drive. This is a significant finding, since it suggests that angular misalignments near the start of the pipe-jack cannot be subsequently corrected. The resulting pipe misalignments are potentially damaging, however, because they are located where the axial jacking loads in the pipe are highest.

2.3 Finite Element modelling of pipe joints

Following the field work described by Norris (1992) a more detailed study of the behaviour of pipe joints was undertaken at Oxford University by Zhou.

This research consisted of Finite Element (FE) studies and physical model testing. The numerical studies were based on the use of two separate finite element programs. Two-dimensional analyses were carried out using OXFEM, developed at Oxford University for the analysis of geotechnical problems. Three-dimensional analyses were also carried out using an elastic finite element program previously developed by Zhou. Data from earlier research results from Stage 1 Ripley (1989) and stage 2 Norris (1992) on joint pressure distributions, pipe strains and failure modes were used to check the validity of the theoretical modelling, from which detailed information on pipe stresses could then be determined.

Results from the early FE analyses allowed the programme of laboratory testing of pipes (described in this report) to be planned and executed.

2.4 Finite Element analyses

The first analyses carried out were of local stresses at a pipe joint, in two dimensions, that included different packing materials and both uniform and eccentric loading regimes. In these analyses the pipe and packer were assumed to be elastic. They were used to demonstrate the effects of varying the stiffness and Poisson's ratio of the packer, and to develop interface elements which would allow a gap to open at the joint as the joint deviation angle increased. These analyses confirmed the importance of Poisson's ratio of the packing material Ripley (1989) and Husein (1989).

Numerical analyses were carried out on a single pipe under localised and diagonal loading. Comparisons between model tests, Ripley (1989) and the FE analyses were generally encouraging.

A numerical model of a single pipe surrounded by elastic ground was then set up, and used to analyse loads acting under field installation conditions recorded from site measurements, Norris (1992). Again agreements between FE analysis and field data were good. As a result of these, and other, calibration exercises it was considered that the numerical models were sufficiently realistic to allow their use for determining detailed stress and strain distributions throughout the pipes.

Results from these analyses indicated that:

- For edge loading, the compressive stresses did not change very much along the pipe and have a distribution close to that obtained from a stocky-column elastic analysis.

- The tensile stresses are small and mainly in the hoop direction.

- For diagonal loading there was a broad band of compressive stress from one loaded area to the other; the tensile stresses were concentrated in a band near the mid line and were mainly caused by bending of the pipe due to loading.

These analyses confirmed the need for hoop reinforcement, even when the main loading is longitudinal.

The final FE analysis phase was to check the end-effects in the single pipe model. To achieve this a three pipe model was analysed. For computational convenience loads were generated by interface stress distributions in the joints. The pipe stresses recorded were not dissimilar from those obtained from the single pipe model.

Zhou also carried out a program of pipe testing at reduced scale. The pipes tested were 232mm long, 200mm in diameter and with a wall thickness of 25mm. All model pipes were tested vertically until failure occurred. Loads were applied by hydraulic jacks through a load cell and a loading platen which was machined flat, to apply uniform loading, or had two bevels machined at a small angle to apply concentrated loads at the pipe joints. The arrangement was symmetrical to overcome the problems of supporting the pipe and plate with eccentric loading; the pipe "barrel" stress therefore differed from the FE analysis, but the local effects at the joint were reasonably realistic.

Tests were conducted on pipes with plain square ends, with various packer arrangements, with profiled ends to reduce stresses at the outside of the pipe, with closely spaced localised hoop reinforcement at the spigot end joint, and with an external prestressing band.

Results from the laboratory testing phase are summarised in Table 2.1. These data confirmed earlier results from the numerical modelling phase and suggested that:

- A profiled joint face chamfer of 2^{o} eliminated spalling of the concrete pipe under working loads.

- The material used for the packer affected the occurrence of spalling and cracking.

- The use of internal closely spaced localised hoop reinforcement or externally placed prestressed steel bands increased the load capacity of the pipe by up to 20%.

The results of the model tests were sufficiently promising that an application for a grant to extend this work was submitted to EPSRC. The grant application was successful, and with financial contributions from the Pipe Jacking Association (PJA) a one-year research programme was undertaken to investigate improvements to the pipe joint details on full scale microtunnelling pipes.

The following sections describes the design of the test rig and modifications incorporated into the standard production DN600 microtunnelling pipes supplied by various manufacturers

Table 2.1 Summary of Laboratory model pipe test results

	NORMALISED STRENGTH (%)		
TEST DETAILS	**Uniform loading**	**Non-uniform loading**	**NOTES**
PLAIN ENDED PIPES			Local spalling and cracking of pipe edges at low loads under non-uniform loading: @ 50% for no packing, @ 30% for rubber packing, @ late stage for plywood packing.
No packing	85	43	
No packing with local reinforcement	-	40	
Rubber packing	55	46,42	
Plywood packing	83	54,54	
Plywood packing, with prestressing	77	61,57	Local spalling greatly reduced
Plywood packing, with local reinforcement	79	62,67	
PIPES WITH PROFILED ENDS			
No packing, with local reinforcement	52	35,44	No local spalling at loads up to failure load
Plywood packing, no reinf't	74	61,57	
Plywood packing, with local reinforcement		63	

Note: Normalised strength = pipe failure load/(pipe section area x concrete cube strength.

3. DESIGN OF MICROTUNNELLING PIPE TEST RIG

3.1 Introduction

This section describes the design of the test rig. Concepts are discussed along with the requirements of the rig

3.2 Design Criteria

The test rig needed to be designed to achieve several criteria. These were:

- The capacity to test DN600 microtunnelling pipes to failure and limit deflection of the rig under maximum loading (6000 kN)
- To be large enough to accommodate a 1.2m long pipe with jacks and load cells.
- Loading platform to be adjustable.
- Capable of testing at a deflection angle (β) of 0.5^{o} and 1.0^{o} maintained throughout the test

The following section describes in detail the design of the test rig with respect to the above design criteria. General arrangements and details of the test rig and pipe platform are presented in Appendix A. Photographs of the test rig with are presented in Plate 3.1.

3.3 Test rig design

3.3.1 Load capacity of test rig

The capacity of the rig was based on the design capacity of a half section of the pipe being loaded. This approach led to a theoretical load of 5130 kN.

The test rig was designed to apply loads up to 6000 kN. This was considered a conservative approach as preliminary calculations carried out by ARC suggested that approximately only 33% and 19% of the pipe area is loaded when a pipe is loaded at a deflection angle of 0.5^{o} and 1.0^{o} respectively. An elastic analysis was then carried out using a structural steel analysis package. Figure 3.1 represents the test rig that was analysed. As a result of the high capacity of the test rig it was felt that relatively large structural steel sections were required. The analysis was run using the following members

Horizontal beam	356 x 406 x 393 Universal column
Vertical stanchions	305 x 305 x 283 Universal column

Figure 3.2 represents the skeletal frame of the test rig analysed and Table 3.1 represents a summary of the results of the analysis data.

It was important to limit central vertical displacement of the horizontal beam and horizontal deflection of the vertical stanchions to minimise rotation of the joints. The critical joints were 1, 14, 15, 16 and 17. To limit deflection a tie rod was introduced between joints 16 and 17.

Results from the analysis indicated that the deflection of joints 1, 14 and 15 was 2.16mm, 1.24mm and 0.9mm respectively. The moment and bending stress at joint 4 was 1000 kNm and 136.9 N/mm^2 respectively. The test rig design was based on these figures.

Design of the stanchion and haunch weld group was based on the maximum moment being applied to joint 4 of 1000 kNm. Consequently a combination of 25mm fillet welds and butt welds were used to weld the stanchion and haunch to the horizontal beam, see Appendix A for details.

Checks were also carried out to assess the stability of the flanges and web of the horizontal beam. These checks consisted of the flange in bending, and the web in tension, compression and for buckling. Checks were also made for web panel shear, however, the web of the horizontal beam failed when a panel shear check was undertaken. This was overcome by welding a 12mm thick plate to the flanges of the horizontal beam to either side, see Appendix A for details.

From the results of the analysis the tie beam between joint 16 and 17 needed to restrain a load of 460 kN. This was achieved by using a Macalloy 460 bar held in place by a block system welded to the web of either stanchion, see Appendix A for details. Each block system was required to have a capacity of 460 kN. To enable the block system to have this capacity, 12mm fillet welds were used throughout, see Appendix A for details.

3.3.2 Accommodation of pipe, jack and load cell

All pipes provided by the manufacturers were 1.2m long with an internal diameter of 600mm. The jacks and load cells used were 305mm and 200mm long respectively. Allowing for a thrust ring, reaction beam and reaction plates a clear spacing of 2150mm between each of the columns of the rig was required

3.3.3 Design of pipe platform

Each pipe was to be tested on a platform independent of the test rig. The platform was required to keep deflection of the platform to a minimum under the self weight of the pipe. The pipe platform consisted of four corner stanchions made from 100 x 100 x 4 square hollow sections attached to two timber beams. These were placed either side of the test rig. Channels were then spanned over the test rig at 100mm centres, details of the pipe platform are included in Appendix A. The deflection of these channels under the weight of the pipe was 0.3mm. This deflection was considered to be insignificant and would not affect the deflection angle of the pipe during testing.

The pipe platform was also designed to stand 15mm clear of the horizontal beam. This allowed the horizontal beam space for deflection without affecting the pipe platform.

Welded to each stanchion is a 20mm thick base plate with four 20mm bolts threaded into the base plate. The bolts give the pipe platform the ability to be levelled both laterally and longitudinally.

3.3.4 Design of reaction beam and reaction plates

The purpose of the reaction beam was to transfer the load to the stanchions. The distance between the two stanchions was relatively small therefore only a short stiff beam was required. The stanchions of the test rig were fabricated from a standard production length of 305 x 305 UC. After the stanchions had been fabricated a length of the universal column remained. This was cut to a size of 900mm and used as the reaction beam This was not only more than stiff enough to transfer the load effectively, but was a relatively economic solution as the length of universal column was waste material.

To enable the pipes to be tested at a deflection angle (β) of 0.5^{o} and 1.0^{o}, chamfered plates were machined to these angles and bolted to the reaction beam for the pipe to be jacked against. The reaction plates were also fabricated in a circular shape to represent an adjacent pipe. For both deflection angles tested two machined reaction plates were fabricated. The first was bolted to the reaction beam with the thickest end placed located so that the bottom of the pipe touches it. A second machined plate (the inverse of the first) was bolted to the first. When both machined reaction plates are placed together a right angle is produced. This is then used to level the pipe in position. Once the face of the pipe is levelled, the second reaction plate is unbolted from the first. The spigot end face of the pipe is therefore then tested at a deflection angle as specified.

Table 3.1 Summary of elastic analysis of test rig

Joint	Moment (kNm)	Vertical Disp. (mm)	Horizontal. Disp (mm)	Bending stress (N/mm2)
1	835.2	2.16445	0	119.3
2	897.0	1.87805	0.09731	128.1
3	773.4	1.80152	0.09589	110.5
4	1000.0	0.89426	0.19391	136.9
5	711.6	0.83730	0.19249	101.7
6	0	0	0.19391	0
7	0	0	0.19249	0
8	720.3	0.89426	0.44552	79.4
9	454.1	0.83730	0.37170	54.9
10	440.5	0.89426	0.70501	623
11	23.9	0.83730	0.55458	35.4
12	160.8	0.89426	0.97160	31.0
13	21.7	0.83730	0.74010	4.2
14	119.2	0.89426	1.24224	27.6
15	169.6	0.83730	0.90447	39.4
16	0	0.89426	1.86766	11.6
17	0	0.83730	1.67530	6.7

4. MODIFICATIONS TO PIPES AND PROGRAMME OF TESTING

4.1 Introduction

After designs of the test rig had been completed various pipe manufacturers were approached and asked to supply DN600 microtunnelling pipes for testing. ARC Pipes, Stanton Bonna Concrete and Hepworths Building Products agreed to supply pipes for testing. This section describes modifications incorporated into these pipes.

4.2 Initial testing considerations

From the laboratory tests carried out by Zhou, it was discovered that hoop reinforcement or external prestressed steel bands at the spigot end improved the load capacity of the pipe. The results also suggested that the inclusion of a 2^{o} joint chamfer could eliminate spalling of the pipe joint at working loads. To confirm these findings the current research project proposed to test these modifications on full scale microtunnelling pipes. To assess the effectiveness of the modifications, comparisons were made with results from standard production pipes.

It was decided to use 600mm internal diameter microtunnelling pipes having a length of 1.2m. This was thought to be large enough to provide a realistic test for all standard jacking pipes, while being manageable in terms of the size and the cost of the test rig. The aspect ratio (length/diameter) is similar to that of larger jacking pipes, typically 1.2 to 1.8m in diameter with a length of 2.4-2.5m. The ratio of the wall thickness to internal diameter of the microtunnelling pipes, however, was significantly larger than that of the larger diameter pipes.

4.3 Phase 1 of the testing programme

ARC Pipes and Stanton Bonna became involved with the research programme during the early stages and agreed to provide twelve DN600 microtunnelling pipes. Although both of these manufacturer's pipes had an external diameter of 765mm there were several significant differences in the pipes. These were:

- ARC pipes were unreinforced, whereas Stanton Bonna pipes were reinforced with a cage of steel located at the middle of the pipe wall

- Stanton Bonna pipes had an internal diameter of 585mm compared to 600mm for ARC pipes. As a result the wall thickness of the Stanton Bonna pipe was slightly greater.

- Spigot joint details were significantly different, Figures 4.1 and 4.3

A summary of the properties of all the standard production pipes tested is given in Table 4.1

After ARC Pipes and Stanton Bonna had agreed to supply pipes for the testing programme an initial meeting was held to discuss the incorporation of the proposed modifications into the manufacturing process. The modifications discussed were the incorporation of hoop reinforcement and the inclusion of a joint chamfer to the spigot end.

4.3.1 Internal hoop reinforcement

Both manufacturers agreed that hoop reinforcement could easily be incorporated into their spinning process. It was agreed that the best approach would be to fabricate a separate cage of reinforcement which could then be placed in the mould for spinning. The reinforcement cage was fabricated using the separate manufacturers' reinforcement cage spiral winding process. The cage of reinforcement was then placed as close to the outside edge of the pipe spigot joint and as close to the end face as possible, Figures 4.2 and 4.4. The proximity of the reinforcement to both the outer and end face was 20mm and 15mm (the manufacturers recommended minimum cover) for Stanton Bonna and ARC pipes respectively. As pipes supplied by Stanton Bonna were already reinforced it was not necessary to manufacture a separate cage of reinforcement. Instead the longitudinal bars of the cage were extended at the spigot end and the spacing of the last 4 hooped bars was reduced.

Figures 4.1-4.4 illustrate the standard pipe joint detail of each pipe manufacturer and the modifications incorporated into each pipe. Plate 4.1 illustrates the cage of reinforcement within the mould of an ARC pipe before spinning commenced.

4.3.2. Joint chamfer

This modification was relatively straightforward to incorporate and involved the spigot forming end plate of the mould being machined to suite the proposed chamfer. Earlier laboratory tests by Zhou had suggested that incorporation of a 2^{o} chamfer to the spigot joint eliminated spalling of the pipe joint at working loads. This chamfer angle was therefore adopted. The pipe manufacturers suggested that each manufacturer could incorporate a different chamfer angle. The effect of variation of chamfer could therefore be assessed. On this basis, it was agreed that pipes produced by Stanton Bonna for the testing programme would incorporate a 2^{o} end joint chamfer and pipes produced by ARC would have a 3^{o} chamfer. For all pipes the chamfer was initiated from the centre of the wall thickness and propagated to the outside edge of the spigot joint, Figures 4.2 and 4.4. A summary of all pipes supplied by ARC and Stanton Bonna is given in Table 4.2

4.4 Phase 2 of the testing programme

After the pipes from ARC and Stanton Bonna had been tested, Hepworths became involved with the research programme. Hepworths also offered to supply twelve DN600 microtunnelling pipes.

Zhou's laboratory work indicated that internal closely spaced hoop reinforcement at the spigot end improved the load capacity of the pipe. The work also demonstrated that externally placed prestressed steel bands at the spigot end also improved the load capacity of the pipe, although, increases in capacity were not as large as for those with hoop reinforcement.

Phase 1 of this testing programme had examined the effect of internal hoop reinforcement. Sufficient time was available after completion of this phase for an additional modification to be investigated. It was therefore decided to study the use of external prestressed steel bands. Two modifications incorporating prestressing bands were proposed. The first included a steel band placed at the end of the spigot joint, Figure 4.6 and Plate 4.2. The second modification consisted of a steel band as described in modification 1 with an additional band placed at the rear of the spigot joint, Figure 4.6 and Plate 4.2

To obtain the required prestressing effect, the diameter of the steel bands needed to be slightly smaller than that of the pipe joint. Prestressing was achieved by heating the steel band, placing it over the joint and allowing it to cool. There were, however, several problems associated with this technique. Firstly, the steel band could not be heated to an excessively high temperature otherwise this could result in damage to the concrete pipe. Secondly, it was unclear how an even heat could be applied to the steel band to allow expansion to occur.

The diameter of the steel band was made 0.5mm smaller than the spigot joint of the pipe. Initial calculations suggested that a temperature of approximately 150^{o}C would cause an expansion of 0.8mm. Contraction of this band would then result in a prestress of approximately 140 N/mm^{2}. Dimensions of the prestressing bands are given in Table 4.3. The stresses listed in Table 4.3 are based on pipe measurements taken at Hepworths pipe works.

The steel bands were fabricated by Barhale Equipment Ltd. An even heat was required to achieve even expansion of the whole steel band. This was achieved by creating a "furnace" on site using an old steel collar from a DN900 jacking pipe filled with timber and coal. This was then ignited and the steel bands placed on the hot coals for a short time. Even expansion occurred and the steel bands were then slipped over the spigot end. Once placed and located water was poured over the heated bands to allow contraction and prestressing to occur. A summary of the pipes supplied by Hepworths is given in Table 4.2

Table 4.1 Properties of the DN600 microtunnelling pipes tested

PIPE PROPERTIES	PIPE MANUFACTURERS		
	ARC Pipes	Stanton Bonna	Hepworths
Overall diameter (mm)	760	760	760
Internal diameter (mm)	600	585	585
Wall thickness at centre of pipe (mm)	80	87.5	87.5
Wall thickness at spigot Joint (mm)	65	67.4	66
Length of pipe (mm)	1200	1195	1200
Reinforced/unreinforced	unreinforced	reinforced (single cage)	reinforced (single cage)
Recommended packer	12mm MDF	18mm Chipboard	15mm MDF
Max. Allowable jacking load @ 0^{o} (tonnes)		254	270
Max. Allowable Jacking load. @ 0.25^{o} (tonnes)		180	216
Max. Allowable Jacking load. @ 0.5^{o} (tonnes)		113	132

Table 4.2 Pipes supplied by manufacturers

Type of pipe tested	**Pipes supplied by manufacturers and deflection angle pipes tested at**					
	ARC Pipes		Stanton Bonna		Hepworths	
	0.5^{o}	1.0^{o}	0.5^{o}	1.0^{o}	0.5^{o}	1.0^{o}
Standard production pipe	1	2	1	2	2	2
Plain end + local reinf't	1	2	1	2		
2^{o} face chamfer			1	1		
3^{o} face chamfer	1	1				
2^{o} face chamfer + local reinforcement			2	2		
3^{o} face chamfer + local reinforcement	2	2				
1 external steel band					2	2
2 external steel bands					2	2

Table 4.3 Dimensions of steel bands and prestressing achieved

	Joint diameter (mm) as measured	**Steel band Internal diameter (mm)**	**Prestress (N/mm2)**
Steel Band 1	717.47	717.0	134
Steel Band 2	737.52	737.0	144

5 DATA ACQUISITION

5.1 Methodologies

Rather than designing a complicated data retrieval system it was decided to keep the system as simple as possible. This was primarily for two reasons. The more complicated the data retrieval system is the longer it takes to get up and running. As the research project was for a period of one year it was felt that time was better spent designing the test rig and carrying out tests. Secondly data were only required to identify whether modified pipes were behaving better than standard production pipes. High precision was therefore not required.

Two pieces of data needed to be recorded. Firstly whether spalling and/or cracking during load application was occurring and at what load. Secondly, a final failure load was required.

The data acquisition system comprised two cameras, various electronic transducers, a monitor, a video recorder and a split screen generator. One of the video cameras was placed under the pipe, within the test rig, during application of load. This enabled the pipe joint to be viewed during application of load. The second camera was then focused onto the two electronic transducers, which in turn were connected to the load cells and displayed a load in kiloNewtons. The signals from both of these cameras were fed into a monitor via a split screen generator. The split screen generator enabled the image of the electronic transducers, displaying the load, to be superimposed on the image of the pipe during loading. This ensured that real time video footage was achieved so that spalling, cracking and failure loads could be determined at a later date. The video images were then recorded. A schematic representation of the data logging equipment is shown in Figure 5.1.

To ensure that the designated deflection angle of the pipe joint was maintained during load application, electro-levels were placed on the reaction beam and the pipe to monitor any angular deflection. Figure 5.2 illustrates the approximate position of the electro-levels. Appendix B tabulates electro-level reading data recorded during testing.

6 TESTS RESULTS

6.1 Results from phase 1 and 2

This section presents results and observations recorded from Phase 1 and 2 of the testing programme. The majority of test data were recorded on video tape during testing of the pipe. It is clearly not possible to present this video footage within this report. However, some typical failure sequences are presented in Appendix C.

Results are tabulated and summarised in a series of tables. Table 6.1 lists the type of pipe tested with an ultimate failure load. Tables 6.2-6.4 presents a detailed account of each pipe failure for each separate pipe manufacturer. Results tabulated include: pipe number (for type of modification incorporated refer to Table 6.1), ultimate failure load, mode of failure (a description of which is given), whether spalling occurred during the application of load, the increase in deflection angle caused by the pipe and reaction beam rotation during testing and any observations made during application of load and after testing was complete.

A full catalogue of photographs of the pipe failures is presented in Appendix D.

An additional two pipes were supplied by Stanton Bonna for a supplementary phase of testing that was outside the scope of the original research programme. The pipes supplied were standard production pipes without the central reinforcement cage. One of these pipes also incorporated a 2^{o} chamfer. Both pipes were tested at a deflection angle of 1.0^{o}. The results are presented in Table 6.3.

Two GRP microtunnelling pipes were supplied by Johnston Pipes. The testing of these pipes were again outside the original scope of the research programme. A detailed description of the failure mechanisms for these pipes are presented in Appendix E.

Table 6.1 Ultimate failure load of pipes tested

TYPE OF PIPE TESTED	FAILURE LOAD (kN)
ARC pipes tested at 0.5°	
Standard production pipe (pipe 1)	2799
Standard pipe with joint chamfer (pipe 2)	2355
Standard pipe with joint reinforcement (pipe 3)	2859
Standard pipe with joint chamfer and reinf't (pipe 4)	2608
Standard pipe with joint chamfer and reinf't (pipe 5)	2635
ARC pipes tested at 1.0°	
Standard production pipe (pipe 6)	2386
Standard production pipe (pipe 7)	2758
Standard pipe with joint chamfer (pipe 8)	2036
Standard pipe with joint reinforcement (pipe 9)	2161
Standard pipe with joint reinforcement (pipe 10)	2661
Standard pipe with joint chamfer and reinf't (pipe 11)	2273
Standard pipe with joint chamfer and reinf't (pipe 12)	2362
Stanton Bonna pipes tested at 0.5°	
Standard production pipe (pipe 1)	3435
Standard pipe with joint chamfer (pipe 2)	3547
Standard pipe with joint reinforcement (pipe 3)	3749
Standard pipe with joint chamfer and reinf't (pipe 4)	3401
Standard pipe with joint chamfer and reinf't (pipe 5)	3428
Stanton Bonna pipes tested at 1.0°	
Standard production pipe (pipe 6)	3240
Standard production pipe (pipe 7)	3198
Standard pipe with joint chamfer (pipe 8)	3148
Standard pipe with joint reinforcement (pipe 9)	3582
Standard pipe with joint reinforcement (pipe 10)	3537
Standard pipe with joint chamfer and reinf't (pipe 11)	3318
Standard pipe with joint chamfer and reinf't (pipe 12)	3154
Standard pipe unreinforced (pipe 13)	2979
Standard pipe unreinforced and 2° chamfer (pipe14)	2908
Hepworth pipes tested at 0.5°	
Standard production pipe (pipe 1)	3502
Standard production pipe (pipe2)	3198
Standard pipe with 1 steel band (pipe 3)	3579
Standard pipe with 1 steel band (pipe4)	3979
Standard pipe with 2 steel bands (pipe 5)	2757
Standard pipe with 2 steel bands (pipe 6)	3100
Hepworth pipes tested at 1.0°	
Standard production pipe (pipe 7)	2942
Standard production pipe (pipe8)	3025
Standard pipe with 1 steel band (pipe 9)	3473
Standard pipe with 1 steel band (pipe10)	3631
Standard pipe with 2 steel bands (pipe 11)	2530
Standard pipe with 2 steel bands (pipe 12)	2873

Table 6.2 Summary of pipe failures for ARC pipes

Pipe No	Failure load (kN)	Mode of failure	Spalling during application of load	Roatation[1] (degrees)	Notes
1	2386	A	No	0.040	Pipe collapsed completely when removed from the test rig.
2	2758	A	No	0.028	
3	2859	B	Yes	0.042	External spalling observed at steel collar end approx. 100-150 kN before failure. Minor cracking observed at spigot end at failure.
4	2608	C	No	0.031	Spalling at the spigot end occurred just before failure.
5	2634	C	No	0.0205	Significant spalling occurred internally at the spigot end just before failure.
6	2386	D	No	0.0295	At failure a large crack occurred above the reaction area of the pipe (i.e. above the reaction beam and plate) see Plate D5, Appendix D.
7	2758	D	No	0.021	External cracks appeared at a load of 2700kN and propagated towards the spigot end. At failure minor cracking around the circumference of the pipe was observed. Minor spalling occurred at the spigot end at failure.
8	2036	A	No	0.026	
9	2161	C	No	0.0425	
10	2661	C	No	0.0325	
11	2273	C	No	0.026	At failure longitudinal cracks that ran the length of the pipe were observed. Localised areas of spalling both internally and externally at the spigot end were also observed.
12	2362	C	No	0.0275	

Description of failure modes

Mode A Explosive failure at the spigot end resulting in large segments of concrete "exploding out" from the sides of the pipe at failure.

Mode B Failure occurred at the steel collar end of the pipe.

Mode C Failure occurred at the spigot end. At failure large segments of concrete became detached from the spigot end revealing the joint reinforcement. The thickness of the concrete segments was approximately half that of the pipe wall at the spigot end.

Mode D Failure occurred at the spigot end. Large longitudinal cracks ran internally the whole length of the pipe around the points of load application.

Notes: 1. Rotation refers to an increase in the deflection angle (β) due to rig and pipe compliance.

Table 6.3 Summary of pipe failures for Stanton Bonna pipes

Pipe No	Failure load (kN)	Mode of failure	Spalling during application of load	Rotation[1] (degrees)	Notes
1	3435	A	No	0.0425	Some spalling observed where two load cells were positioned.
2	3546	B	No	0.0325	A section of pipe failed internally at the spigot end.
3	3749	A	No	0.026	At failure large cracks and sections of the concrete pipe became detached at the steel collar end. A small section of concrete pipe also became detached from the spigot joint, see Plate D13, Appendix D.
4	3401	B	No	0.0275	As the failure zone moved further away from the spigot joint the thickness of the detached concrete segments reduced in thickness to approx. 10mm.
5	3428	A	No	0.0355	
6	3240	B	No	0.034	
7	3198	B	No	0.037	The failure zone one side extended for over half the length of the pipe.
8	3148	B	No	0.037	
9	3582	A	No	0.0365	Large segments of concrete, approximately 5mm thick, fell from the external part of the pipe at failure. No internal spalling was observed.
10	3537	A	No	0.042	No internal spalling was observed at failure.
11	3318	B	No	0.031	
12	3154	B	No	0.0365	
13	2979	C	No	-	At a load of approx. 2400kN two large longitudinal cracks occurred that ran the length of the pipe initiaing from the spigot end. At failure a large segment of concrete fell from the top of the pipe, see Plate D23, Appendix D
14	2908	C	No	-	As above except cracks occurred at a load of 2150kN and no large segment of concrete fell from the top of the pipe, only a large crack was observed.

Description of failure modes

Mode A Failure occurred at the steel collar end.

Mode B Failure occurred at the spigot end. At failure large segments of concrete became detached from the spigot end revealing the central reinforcement cage. This created a failure zone that was initiated from the spigot end and propagated towards the steel collar end. The thickness of the concrete segments was approximately half that of the pipe wall at the spigot end.

Mode C Explosive failure at the spigot end resulting in large segments of concrete "exploding out" from the sides of the pipe at failure.

Notes: 1. Rotation refers to an increase in the deflection angle (β) due to rig and pipe compliance.

Table 6.4 Summary of pipe failures for Hepworth pipes

Pipe No	Failure load (kN)	Mode of failure	Spalling during application of load	Notes
1	3502	A	No	
2	3198	B	No	
3	3579	C	No	Several large cracks that were initiated from the spigot joint were observed at failure. Some spalling occurred internally at failure.
4	3979	B	No	Prior to failure the weld of the steel band failed causing the band to be thrown from the spigot joint. As a result a failure mode B was observed.
5	2757	D	No	
6	3100	D	No	Small segments of concrete became detached from the spigot end at failure. Internal and external spalling occurred at the steel collar end at failure.
7	2942	A	No	
8	3025	A	No	
9	3473	B	No	
10	3631	C	No	
11	2530	D	No	
12	2873	D	No	

Description of failure modes

Mode A Failure occurred at the steel collar end.

Mode B Failure occurred at the spigot end. At failure large segments of concrete became detached from the spigot end revealing the central reinforcement cage. This created a failure zone that was initiated from the spigot end and propagated towards the steel collar end. The thickness of the concrete segments was approximately half that of the pipe wall at the spigot end.

Mode C Failure occurred at the spigot end. At failure segments of concrete became detached from the spigot end. These segments were not as large as those described in the Mode B. The prestressed steel band kept the pipe together at failure.

Mode D Failure occurred at the spigot end. At failure several cracks were initiated from the spigot end. No segments of concrete became detached from the pipe at failure. Minor cracking around the circumference of the spigot joint, between the two steel bands was observed at failure.

7. DISCUSSION OF RESULTS

7.1 Introduction

Test data recorded during pipe testing is discussed in this section. The mode of failure observed from the video footage recorded is also discussed. Typical failure sequences from the video footage are presented in Appendix D.

Each manufacturer's set of pipes is discussed separately. Comparisons are made between pipes with modifications and standard production pipes. Discussions are made in the context of:

- Effect of joint modification on the failure load of the pipe
- Effect of joint modification on preventing cracking/spalling during application of load

7.2 Results from phase 1

7.2.1 ARC pipes

7.2.1.1 Standard production pipe tested at 0.5^{o} and 1.0^{o}

A single standard production pipe was tested at a deflection angle of 0.5^{o}. The failure load of this pipe was 2779 kN. At a deflection angle of 1.0^{o} two standard production pipes were tested. The average failure load of these two pipes was 2572 kN. The difference between failure loads of pipes tested at 0.5^{o} and 1.0^{o} is surprisingly small. An analysis carried out using a software package at ARC pipes, based on the PJA "Guide to Best Practice for the installation of Pipe Jacks and Microtunnels" June 1995, suggested that the failure load of the pipe tested at 1.0^{o} is half that of the pipe tested at 0.5^{o}. This relatively small measured difference between the failure loads at different values of β was observed throughout this project..

A possible explanation for this phenomenon is that during the application of load the pipe and/or reaction beam moves. This movement could, in the worst case reduce or increase the deflection angle so that all pipes are tested at a similar deflection angle. This would ultimately result in similar failure loads being recorded for all pipes. This movement, however, was anticipated prior to testing. Electro-levels were therefore strategically placed to monitor these movements, refer to section 5. Electro-level readings during testing are presented in Appendix D. Tables B1, B6 and B7, Appendix B are the Electro-level (EL) results for the Standard production pipes tested at 0.5^{o} and 1.0^{o}. EL1 and EL2 were placed either end of the pipe during testing. The average of these two electro levels is the rotation of the pipe. Electro level 3 was placed in the reaction beam on the centre line of the pipe. During testing the pipe always moved in an upward direction at the reaction beam end of the rig. Upward movements of the pipe decreased with increasing load. This was the case for all pipes tested and is clearly seen

for the electro-level results in Appendix B. The upward movement of the pipe was generally more significant up to a load application of 500 kN.

During application of load the reaction beam also moved. Unlike the pipe the reaction beam moved in a downward direction. This downward movement was also more pronounced during the early stages of load application. After a load of approximately 500 kN movement was less significant.

The overall effect of the deflection angle is calculated by subtracting the reading of EL3 from the average of EL1 and EL2. As can be seen from Tables B1, B6 and B7 the overall effect of the pipe and reaction beam movement equated to a positive angular movement of between 0.021^{o} and 0.0295^{o} (i.e. the movement of the pipe during load application being slightly more significant). Therefore the pipe tested at 0.5^{o} was actually tested at 0.528^{o} at approximately failure. The pipes tested at a deflection angle of 1.0^{o} were tested at a deflection angle of 1.0295^{o} and 1.021^{o} at approximately failure. This movement during testing was considered insignificant and would certainly not account for the small difference in the load recorded between pipes tested at 1.0^{o} and 0.5^{o}.

Before any testing commenced, a packer material was placed between the spigot end of the pipe and the machined reaction plate. During the application of load this material compressed resulting in a more even distribution of the stresses around the loaded area of the pipe joint. This ability to compress and spread the load evenly may explain why relatively small differences occur between the failure loads of pipes tested at a deflection angle of 0.5^{o} and 1.0^{o}.

The analysis of video footage revealed that spalling did not occur during application of load at the spigot end. Occasionally cracking was observed, although, this always occurred just before failure. In contrast previous work carried out by Zhou on model pipes suggested that spalling occurred at relatively low loads. The testing methodology adopted by Zhou was, however, significantly different to the method adopted for this project. The most significant difference was the method used for testing pipes at different deflection angles. Zhou tested pipes vertically in a compression machine. A platen was placed on top of the pipes that had been machined either side to generate a small deflection angle. The arrangement was symmetrical and resulted in opposite sides of the spigot joint being tested. This resulted in a "barrel" failure mode being recorded. Pipes tested in this research project were, however, only loaded on one part of the pipe. Failure mechanisms were therefore significantly different which may explain the lack of spalling during loading compared to observations made by Zhou.

An "explosive" failure of all standard production pipes occurred. This was an expected result as the pipes tested were unreinforced.

7.2.1.2 Pipes with a 3^{o} joint chamfer tested at 0.5^{o} and 1.0^{o}

A single pipe was tested at each deflection angle. The failure load of the pipe tested at a 0.5^{o} was 2355 kN compared with the failure load of 2036 kN for the pipe tested at 1.0^{o}.

The difference in failure loads was 319 kN. This again is relatively small and is thought to be associated with the effectiveness of the packer material.

The reduction in load capacity for pipes tested at 0.5^{o} and 1.0^{o} compared to the corresponding standard production pipe was 15.3% and 20.8% respectively. The reduction in load was expected as the loaded area of the pipe is significantly reduced due to the chamfer. The chamfer was primarily included to eliminate spalling during application of load. No spalling or cracking was observed visually or from video footage during the application of load, although, this was also the case for standard production pipes tested.

An "explosive" mode of failure occurred due to the tested pipes being unreinforced.

7.2.1.3 Pipes with local joint reinforcement tested at 0.5^{o} and 1.0^{o}

The failure load of the pipe tested at a deflection angle of 0.5^{o} was 2859 kN, 2.9% greater than the failure load of the standard production pipe. For the two pipes tested at a deflection angle of 1.0^{o} the average failure load recorded was 2411 kN. This was a reduction of 6.3% when compared to the average failure load of a standard production pipes.

When the pipe is loaded at a deflection angle high localised stresses are encountered at the ends of the pipe. The effect of the localised stress is more significant at the spigot end as the wall thickness is thinnest here. The inclusion of reinforcement within the spigot end will therefore increase the load capacity of the pipe. This was demonstrated for the pipe tested at 0.5^{o}, although, the average failure load of the two pipes tested a deflection angle of 1.0^{o} demonstrated a decrease in load capacity.

A possible explanation for this is the difference between the failure loads of the two pipes tested at 1.0^{o}. One pipe failed at a load of 2161 kN. The second pipe tested, however, failed at a load of 2661 kN, a difference of 500 kN. After testing of the first pipe was complete it was noted that the machined reaction plate was incorrectly attached to the reaction beam. This resulted in the pipe being tested at a greater deflection angle than intended. Consequently the failure load of the pipe was reduced. If the first test is disregarded and only the second considered then the failure load is 3.4% greater than the standard production pipe. This percentage increase in strength is of a similar magnitude to that of the pipe tested at a deflection angle of 0.5^{o}. A further test is required to ascertain the effect of the incorrect placement of the reaction plate on the failure load.

The pipes tested at a deflection angle of 0.5^{o} failed at the steel collar end of the pipe rather than at the spigot end. As the wall of the pipe is thicker at the steel collar end of the pipe compared with the spigot end the load bearing capacity is considerably greater. The failure mode at the steel collar end was therefore considered unusual. Possible reasons for this failure mode occurring were;

1. The thrust ring placed at the steel collar end of the pipe was incorrectly placed or was not stiff enough to distribute load sufficiently.

2. The inclusion of joint reinforcement strengthened the spigot joint considerably resulting in failure occurring at the steel collar end.

When the pipe was inspected after failure it was noted that localised areas of spalling had occurred both internally and externally. Spalling had also occurred approximately where loading had been applied, see plate D2, Appendix D. This suggested that the unusual result was a direct result of the thrust ring being incorrectly positioned rather than the joint reinforcement causing a "super" strengthening of the spigot joint.

7.2.1.4 Pipes with local joint reinforcement and 3^{o} chamfer tested at 0.5^{o} and 1.0^{o}

At each deflection angle two pipes were tested. The average failure load for pipes tested at a deflection angle of 0.5^{o} and 1.0^{o} was 2611 kN and 2318 kN respectively. The difference in failure loads of the pipes tested at 0.5^{o} and 1.0^{o} was only 293 kN. This small difference is likely to be a result of the effectiveness of the packer material.

Compared to the standard production pipe the load capacity of the pipe decreased by 6.0% and 9.9% for pipes tested at a deflection angle of 0.5^{o} and 1.0^{o} respectively. This reduction in load capacity is a result of the chamfer at the spigot end as discussed earlier in section 7.2.1.2. However, when compared to the failure load of the pipes with a 3^{o} chamfer an increase in load capacity was recorded. The increase in load capacity was 9.8% and 12.9% respectively for pipes tested at a deflection angle of 0.5^{o} and 1.0^{o}. This increase in strength was due to the local joint reinforcement.

At failure large segments of concrete pipe became detached from the underside of the spigot joint exposing the joint reinforcement. Unlike the standard production pipe where an "explosive" mode of failure was observed the reinforcement in the spigot joint had the affect of keeping the pipe intact at failure, see plates D3, D4, D8 and D9, Appendix D. During the application of load no cracking or spalling was observed at the spigot end of the pipe. Any cracking that was noted occurred just before failure of the pipe when segments of concrete became detached from the body of the pipe.

7.2.2 Stanton Bonna pipes

7.2.2.1 Standard production pipe tested at 0.5^{o} and 1.0^{o}

The pipe tested at a deflection angle of 0.5^{o} failed at a load of 3435 kN. The two pipes tested at 1.0^{o} failed at 3240 kN and 3198 kN giving an average failure load of 3219 kN. The difference in load between the pipes tested at different deflection angles is only 6.3%. Insignificant movement of the pipe and reaction beam suggested that the effectiveness of the packer material may explain this relatively small difference in load capacity, as discussed in section 7.2.1.1

No cracking or spalling was observed during the application of load. Any cracking observed during testing occurred just before failure of the pipe.

The pipe tested at a deflection angle of 0.5° failed at the steel collar end of the pipe. Examination of the pipe after failure revealed that failure was initiated at the part of the pipe where loading was applied, plate D11, Appendix D. This suggests that the failure at the steel collar end was a result of the thrust ring being incorrectly placed in the pipe, thus causing high localised stresses as discussed earlier in section 7.2.1.3

Pipes tested at a deflection angle of 1.0° failed at the spigot end. At failure segments of concrete became detached from the spigot end exposing the central cage of reinforcement, plates D16 and D17, Appendix D. This failure zone was initiated at the spigot end. The cage of reinforcement therefore kept the pipe intact at failure, unlike the pipes manufactured by ARC which were unreinforced and where an explosive mode of failure was observed

7.2.2.2 Pipes with a 2° joint chamfer tested at 0.5° and 1.0°

A single pipe was tested at both deflection angles. The failure load of the pipe tested at 0.5° was 3547 kN compared with a failure load of 3148 kN for the pipe tested at 1.0°, a difference of only 399 kN. Insignificant movement of the pipe and reaction beam during testing suggested that the relatively small difference in failure loads was a result of the effectiveness of the packing material.

The failure load of the pipe tested at a deflection angle of 1.0° was 2.3% less than the failure load of the standard production pipe confirming the earlier findings. This confirmed the findings from tests carried out on ARC pipes with a 3° chamfer. However, the reduction in load capacity was considerably greater when a 3° chamfer was incorporated compared to a 2° chamfer.

However, when the failure load of the pipe tested at 0.5° was compared with the failure load of the standard production pipe the reverse was noted. At this deflection angle the load capacity of the pipe had increased by 3.2% when compared with the standard production pipe. This was an unexpected result as reductions in load capacity were expected. Electro-level readings, Table B14, Appendix B, indicate that pipe and reaction beam movement was insignificant during load application and therefore would not effect the failure load. It is unclear why a greater failure load was recorded, although, it is possible that the pipe was incorrectly set up prior to testing.

No cracking or spalling was observed during the application of load. Any cracking observed during testing occurred just before failure of the pipe was induced.

7.2.2.3 Pipes with local joint reinforcement tested at 0.5° and 1.0°

A single pipe was tested at a deflection angle of 0.5°. The failure load of this pipe was 3749 kN, an increase in load capacity of 9.1% when compared to the standard production pipe. Two pipes were tested at a deflection angle of 1.0°. The failure load for these pipes were 3582 kN and 3537 kN giving an average failure load of 3560 kN. This was a 10.6% increase in load capacity when compared to the standard production pipe. The increase in load capacity for Stanton Bonna pipes was more significant than the increase recorded for ARC pipes. Insignificant movement of the pipe and reaction beam

during testing suggested that the relatively small difference in failure loads was a result of the effectiveness of the packing material.

All pipes with local joint reinforcement failed at the steel collar end of the pipe. Examination of the pipes after failure indicated that spalling of the concrete pipe had occurred externally, and in some cases internally, where application of loading occurred. As discussed previously, this failure mode was likely to be a result of incorrect placement of the thrust ring causing an uneven distribution of load at the steel collar end of the pipe. However, as all three pipes had failed at the steel collar end it was possible that the placement of the four closely spaced bars, acting in combination with the existing central cage of reinforcement, led to the spigot end becoming stronger than the steel collar end of the pipe. Closer inspection of the thrust ring, however, revealed that the ring had been damaged during testing. This therefore led to the load being unevenly distributed at the steel collar end causing high localised areas of stress leading ultimately to failure. Before phase 2 of the testing programme was carried out another thrust ring was manufactured to overcome this problem.

No cracking or spalling was observed during the application of load. Any cracking observed during testing occurred just before failure of the pipe was induced.

7.2.2.4 Pipes with local joint reinforcement and 2^{o} chamfer tested at 0.5^{o} and 1.0^{o}

At each deflection angle two pipes were tested. The average failure load for pipes tested at a deflection angle of 0.5^{o} and 1.0^{o} was 3415 kN and 3236 kN respectively. This was a decrease in load capacity of 0.6% and 0.1% for pipes tested at 0.5^{o} and 1.0^{o} respectively compared to the load capacity of the standard production pipe. This reduction in load was relatively insignificant compared to the reduction in load capacity of ARC pipes with joint reinforcement and a 3^{o} chamfer.

When compared to the failure load of the pipes tested with only a 2^{o} chamfer angle the load capacity of the pipes tested at 1.0^{o} increased by 2.8%. This increase in strength was expected and was due to the local joint reinforcement. For pipes tested at 0.5^{o} a decrease in load capacity of 3.7% was recorded compared to the pipe tested with a 2^{o} chamfer, however, it is unclear why this reduction occurred

No cracking or spalling was observed during the application of load. Any cracking observed during testing occurred just before failure of the pipe was induced.

7.2.2.5 Standard production pipes (unreinforced)

Two additional pipes were supplied by Stanton Bonna. Both of these pipes were unreinforced, but had different joint profiles. One of the pipes incorporated a 2^{o} joint chamfer whereas the other had the standard joint profile. Although these pipes were outside the scope of the research a brief discussion is presented below.

Both pipes were tested at a deflection angle of 1.0^{o}, failure occurred at the spigot end of the pipe. At failure large segments of concrete "exploded" out from the pipe, see plates D23 and D24, Appendix D. This mode of failure observed was similar to that observed

for the standard production pipe manufactured by ARC pipes (this also was unreinforced).

During testing large longitudinal cracks appeared that ran the extent of the pipe. These cracks occurred at a load of approximately 2400 kN for the pipe with a standard joint profile and approximately 2150 kN for the pipe with a 2^{o} joint chamfer. The occurrence of these cracks were significant enough to classify that a failure had occurred. Application of load, however, continued until an "explosive" mode of failure occurred. For both pipes an explosive failure occurred at a load of 2908 kN and 2979 kN. The average of these two loads was 8.6% lower than the load capacity of the standard production pipe. This is not a significant reduction in strength, however, if the occurrence of the longitudinal cracks is considered to constitute failure then the average of these failure loads is 29.3% less than the failure load of the standard production pipe. This percentage reduction is more significant.

No cracking or spalling was observed during the application of load. Any cracking observed during testing occurred just before failure of the pipe was induced.

7.3 Summary discussion of Phase 1 test results

For part of the testing programme only a single pipe was tested. Ideally more tests are required so that a reasonable statistical average is achieved. Some duplicate testing was carried out on certain pipes. The difference between failure loads of the two pipes tested were generally very small compared to the overall failure load. This gave a certain degree of confidence that the failure load of the single pipe was a reasonable value of the likely failure load. Bearing this in mind several trends became apparent from the test data. These were:

- Earlier work carried out by Zhou suggested that spalling at working loads could be eliminated by incorporating a chamfered spigot joint. During testing of the pipes with a joint chamfer no spalling was observed during the application of load, although, this was the case for all pipes tested. There were significant differences between the testing methodologies adopted in this research programme compared to those adopted by Zhou which may explain the different results.

- The inclusion of a chamfered joint profile generally reduced the load capacity of the pipe when compared to the load capacity of the standard production pipe. A greater reduction in load capacity was recorded for pipes with a 3^{o} chamfer compared to pipes with a 2^{o} chamfer. The inclusion of a joint chamfer would therefore appear to be detrimental.

- When joint reinforcement is placed at the spigot end of the pipe with a joint chamfer the load capacity is increased. However, generally this increase is not sufficient to produce a pipe that has a greater load capacity than the standard production pipe.

- When joint reinforcement is added to the standard production pipe the load capacity of the pipe increased. The increase in capacity ranged from 1.0% to 9.9% depending

upon type of pipe and deflection angle at which the pipe was tested. This supports earlier work carried out by Zhou. However, the increase reported by Zhou was greater than that reported here. Possible reductions in manufacturing costs could therefore be made by reducing the lightly stressed reinforcement in the "barrel" of the pipe and increasing the joint reinforcement at the spigot end. Further work is required to optimise the arrangement of joint and barrel reinforcement to obtain a sensible balance between increase in load capacity and reduction in manufacturing costs.

- The relatively small difference in failure loads between pipes tested at 0.5^{o} and 1.0^{o} would appear to be a result of the effectiveness of the packer material compressing and distributing the load evenly. Electro-level readings taken during testing indicated that pipe and reaction beam movement was insignificant during the application of load.

- An "explosive" failure mode was observed for pipes that were unreinforced, whereas pipes with a central cage of reinforcement held together at failure.

7.4 Phase 2 test results

7.4.1 Hepworth pipes

7.4.1.1 Standard production pipes tested at 0.5^{o} and 1.0^{o}

Two pipes were tested at each deflection angle. The average failure load of the pipes tested at 0.5^{o} was 3350 kN compared with 2984 kN for pipes tested at 1.0^{o}. The difference between failure loads at different deflection angles was again smaller than anticipated and is likely a result of the effectiveness of the packing material compressing and transferring the load evenly. No electro-level readings were taken during phase 2 of the testing programme as a malfunction occurred in all 3 electro-levels at the on-set of the testing phase.

One of the pipes tested at a deflection angle of 0.5^{o} failed at the spigot end whereas the other failed at the steel collar end of the pipe. Both pipes tested at a deflection angle of 1.0^{o} failed at the steel collar end of the pipe. Failure induced at the steel collar end is likely to be a result of the incorrect placement of the thrust ring as localised spalling and failure was noted at the point of application of load, see plate D25 and D31, Appendix D.

For all pipes tested no cracking or spalling was observed during the application of load. Any cracking observed during testing occurred just before failure of the pipe was induced. When failure occurred at the spigot end of the pipe tested at 0.5^{o} large segments of concrete became detached from the underside of the pipe revealing the central cage of reinforcement. This created a "failure zone" that was initiated at the spigot end, see plate D26, Appendix D. The reinforcement cage tended to keep the pipe intact at failure. This was a was similar failure mode to that described for Standard

production pipes supplied by Stanton Bonna and pipes supplied by ARC with local joint reinforcement.

7.4.1.2 Pipes with one prestressed steel band tested at 0.5^{o} and 1.0^{o}

Two pipes were tested at each deflection angle. The average failure load of pipes tested at 0.5^{o} was 3779 kN compared with 3553 kN for pipes tested at 1.0^{o}. Compared to the failure load of the standard production pipe tested at the corresponding deflection angle this represented an increase in load capacity of 19.1% and 12.8% for pipes tested at 0.5^{o} and 1.0^{o} respectively. The increase in load capacity was significantly greater than the increase reported for joint reinforcement. This was surprising as earlier model testing conducted by Zhou had reported that improvements in load capacity were achieved with both internal and external joint reinforcement, however, internal reinforcement proved more successful.

The failure mode of all pipes with a single external prestressed band was significantly different to that observed for the standard production pipes. At failure large cracks were initiated from the spigot end. Smaller segments of concrete also became detached from the underside of the spigot end. For one pipe tested at a deflection angle of 0.5^{o} the steel band broke and was propelled from the spigot joint. This resulted in large segments of concrete becoming detached from the underside of the spigot joint revealing the cage of central reinforcement. This mode of failure was the same as that observed for the standard production pipe. The external prestressed band therefore not only increased the load capacity, but also prevented a pipe collapse at the spigot end of the pipe at failure.

No cracking or spalling was observed during the application of load. Any cracking observed during testing occurred just before failure of the pipe was induced.

7.4.1.3 Pipes with two prestressed steel bands tested at 0.5^{o} and 1.0^{o}

Two pipes were tested at a deflection angle of 0.5^{o} and 1.0^{o}. The average failure load for pipes tested at 0.5^{o} and 1.0^{o} was 2929 kN and 2702 kN respectively. These results were surprising for two reasons. Firstly, when compared to the failure load of the pipes tested with one prestressed steel band a reduction in load capacity occurred. This reduction in load capacity was 22.5% for pipes tested at 0.5^{o} and 23.9% at 1.0^{o}. This was a considerable decrease in load capacity. Even more surprising was the fact that the load capacity of the pipes was significantly less compared to the standard production pipes. The percentage reduction in load capacity for pipes tested at 0.5^{o} and 1.0 was 12.6% and 9.5% respectively.

For all pipes tested failure occurred at the spigot end of the pipe. The mode of failure for the pipes was significantly different compared to standard production pipes and pipes with a single prestressed steel band. No cracking or spalling was observed during the application of load. When failure occurred some spalling was observed at the spigot end along with some crack patterns. These cracks were generally longitudinal and were located between the two steel bands, see plates D29, D35 and D36 Appendix D. At the extreme edge of the spigot joint no damage or cracking was observed. Some longitudinal cracks were also observed outside the steel bands in the main body of the

pipe, however, these were minor compared to the cracks observed between the steel bands, see plates D29, D35 and D36, Appendix D. Cracking around the circumference of the spigot joint was also observed between the two steel bands.

These crack patterns suggest that failure of the pipe occurred between the two steel bands at the spigot end. This mode of failure is possibly a result of the two steel bands being closely spaced. As load is applied a Poisson's expansion of the pipe occurs causing a further prestressing of the steel bands. Expansion of the pipe between the two steel bands is also restricted due to the increase in prestressing of the steel bands. As load application increases the prestressing effect is increased further until stresses induced by the steel bands are more significant than the stress generated from compressive forces. As a result failure is induced between the steel bands. Further testing using numerical methods are required so that a better understanding of the failure mechanism can be achieved

Although load capacity of the pipe was significantly reduced when two prestressed steel bands were placed at the spigot end the pipe remained virtually intact at failure.

7.4.2 Summary discussion of phase 2 results

Phase 2 of the testing programme was significantly different to phase 1. Joint profiles were not incorporated into the pipes provided by Hepworths as results from phase 1 suggested that the load capacity of the pipe was reduced significantly as a consequence. External prestressed steel bands were placed at the spigot joint in place of the internal joint reinforcement adopted in phase 1. Several trends became apparent from the results. These were:

- The incorporation of a single prestressed steel band improved the load capacity of the pipe considerably. Improvements in load capacity were significantly better than those reported in phase 1 for internally placed reinforcement at the spigot joint. These results were better than expected as previous work suggested that externally placed prestressed bands were not as successful as internal joint reinforcement. The use of external prestressed steel bands has several advantages over the placement of internal joint reinforcement. Firstly, the spinning process does not have to be modified, which can be a costly exercise. Secondly, the steel bands can be used relatively easily as a retro-fit on site when problems occur with jacking load capacities. Heating of the steel band on site to achieve even expansion could, however, be difficult. Further work is therefore required to investigate the effect of an external band that can be placed over the spigot joint without heating (i.e. a steel band approximately the same size as the spigot joint). Further work is also required to optimise the position of the steel band.

- When two steel bands were incorporated at the spigot end the load capacity was reduced considerably compared to the standard production pipe.

- The central cage of reinforcement in the standard production pipe kept the pipe intact at failure except for a failure zone that was initiated from the spigot end. In this failure zone large segments of concrete became detached from the pipe at the

spigot end revealing the central cage of reinforcement. This was a similar mode of failure to that observed in phase 1 of the testing programme.

8. CONCLUSIONS AND RECOMMENDATIONS FOR FURTHER WORK

Earlier work carried out by Zhou on model pipes suggested that spalling of a pipe joint at working loads could be eliminated and the jacking load could be increased through relatively minor modifications to the pipe joint profile and reinforcement details.

This project has extended this previous work and carried out tests on pipes at full scale. Pipes tested were DN600 microtunnelling pipes and were supplied by ARC Pipes, Stanton Bonna Concrete and Hepworth Building Products. Pipes were tested at a deflection angle of 0.5^{o} or 1.0^{o} with various modifications incorporated into the spigot joint end of the pipe. The modifications included a profile joint chamfer, localised joint reinforcement (either external or internal) or a combination of a joint chamfer and joint reinforcement. Comparisons between failure loads and mechanisms of standard production pipes and modified pipes were made and the following conclusions were made.

Previous work suggested that a chamfered joint profile at the spigot joint of a pipe may help to eliminate spalling of the joint during the application of load. During loading of all pipes, including those with a joint chamfer no spalling was observed until failure occurred. The introduction of a joint chamfer generally reduced the capacity of the pipe by between 2.3% and 20.8% when compared to a standard production pipe. The angle of joint chamfer also affected the decrease in load capacity. Reductions in load capacity for pipes incorporating a 2^{o} chamfer were less significant compared to a pipe with a 3^{o} chamfer. The inclusion of a joint chamfer would therefore appear to be detrimental.

When internal hoop joint reinforcement was included in the spigot end of pipes with a joint chamfer an increase in load capacity was observed. However, the load capacity of the pipe was generally less than the load capacity of a standard production pipe.

The load capacity of the pipe was increased when closely spaced internal hoop reinforcement was placed in the spigot joint of the pipe when compared with a standard production pipe. The increase in load capacity was between 1% and 9.9%. This increase was not as significant as that recorded by Zhou, but would support the finding that barrel reinforcement could be reduced if a cage of closely spaced reinforcement is placed at the spigot end. Production costs could therefore be reduced slightly. Further work is needed to obtain the optimum reduction in barrel reinforcement and the optimum joint reinforcement to obtain maximum savings in cost and maximum increases in load capacity.

The incorporation of a single externally placed prestressed steel band at the spigot joint increased the load capacity of the pipe by up to 19% when compared to a standard production pipe. The increase in load capacity was more significant than that observed when internal joint reinforcement was used and contrasted with earlier work carried out by Zhou. An external steel band is a relatively simple modification to incorporate and could be used as a retro-fit on site when jacking problems arise, although, heating the steel band to generate even expansion may be difficult. Further work is required to optimise the positioning of the steel band, and to investigate improvements, if any, by

using a steel band that can be placed over the spigot end without the need for preheating.

When two prestressed bands were placed at the spigot joint the load capacity of the pipe was significantly less than that of the standard production pipe by as much as 12.8%.

The research project was concerned with pipes with an internal diameter of 600mm and 1.2m long. It is unclear how the results described in this report relate to pipes of a different size. The main findings of this research are (a) joint chamfers are not effective, (b) joint reinforcement has a useful role in improving performance and (c) an external steel band placed at the spigot end may have a highly beneficial effect. It seems likely that these broad findings would be applicable to pipes of different sizes. In order to investigate this further, additional testing would be required.

The research has highlighted certain areas where definite improvements can be made in the design of microtunnelling pipes. However, further full scale testing and numerical analysis is required to optimise the modifications investigated.

REFERENCES

Husein, N. A. (1989) "Vitrified Clay Pipes Installed by Trenchless Techniques". Ph.D. Thesis, University of Bradford.

Norris, P. (1992) "The Behaviour of Jacked Concrete Pipes During Site Installation". D.Phil. Thesis, University of Oxford.

Ripley (1989) "The Performance of Jacked Pipes. D.Phil. Thesis, University of Oxford.

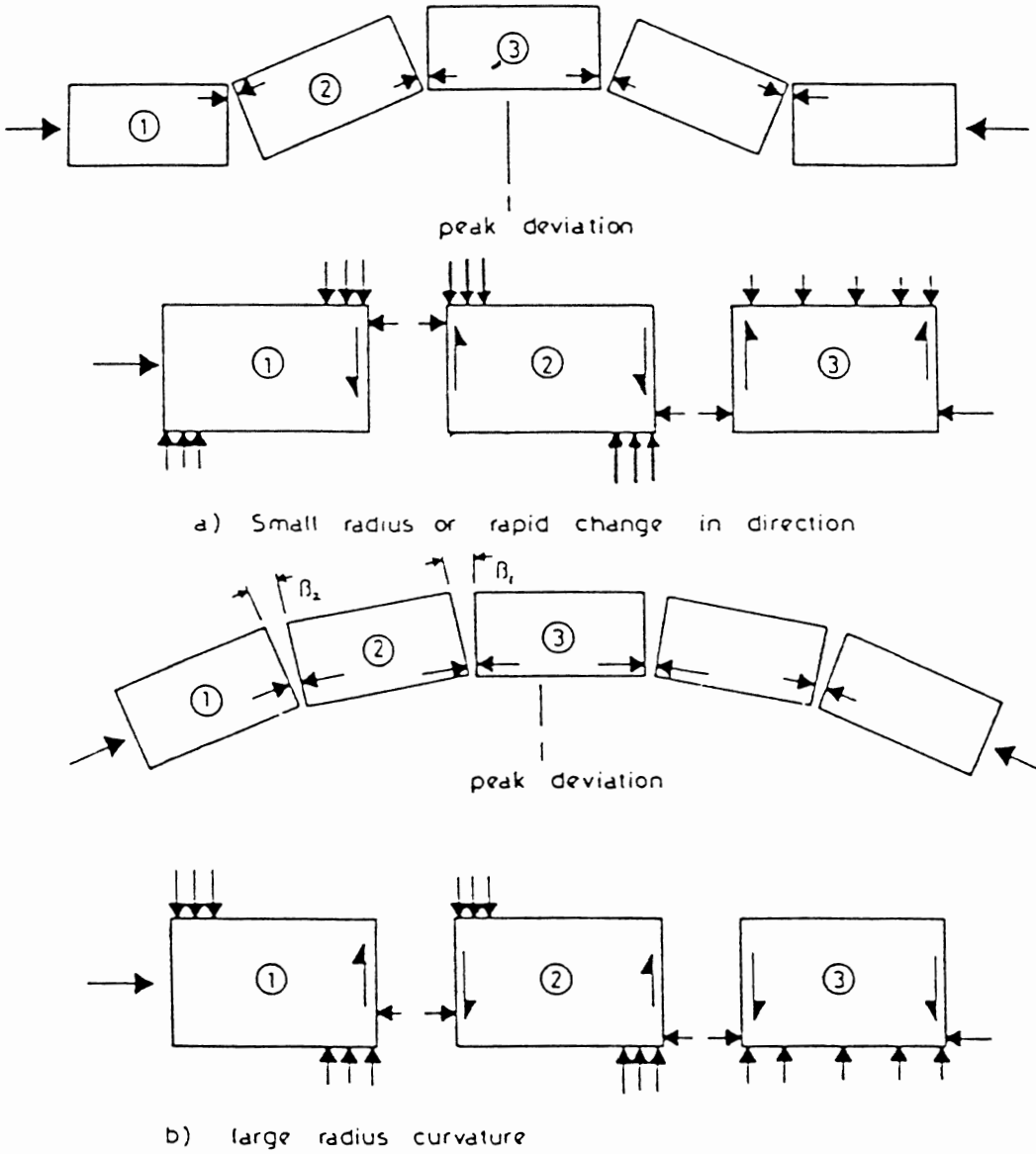

Figure 2.1 Theoretical misalignment forces

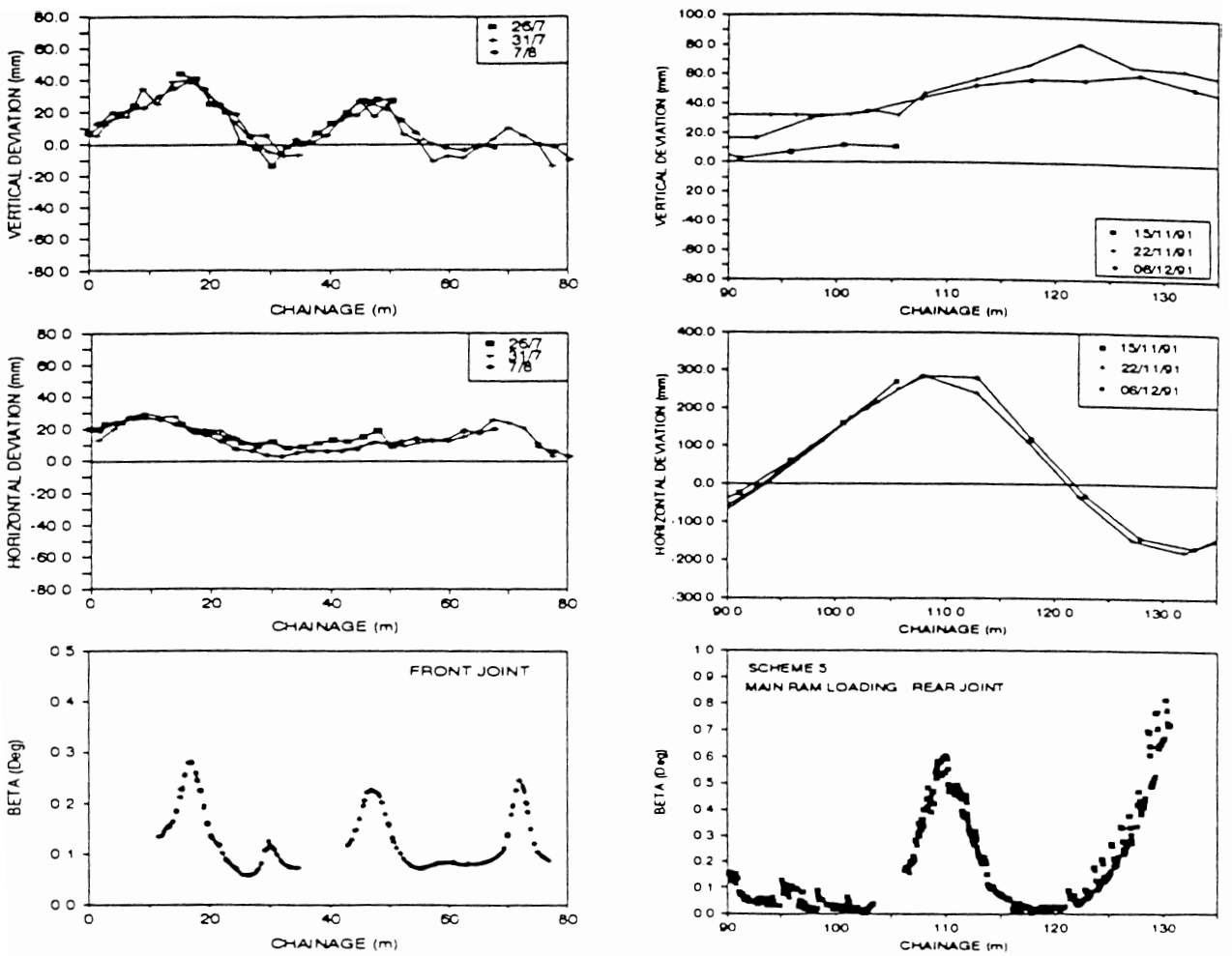

Figure 2.2 Tunnel alignment data (after Norris 1992)

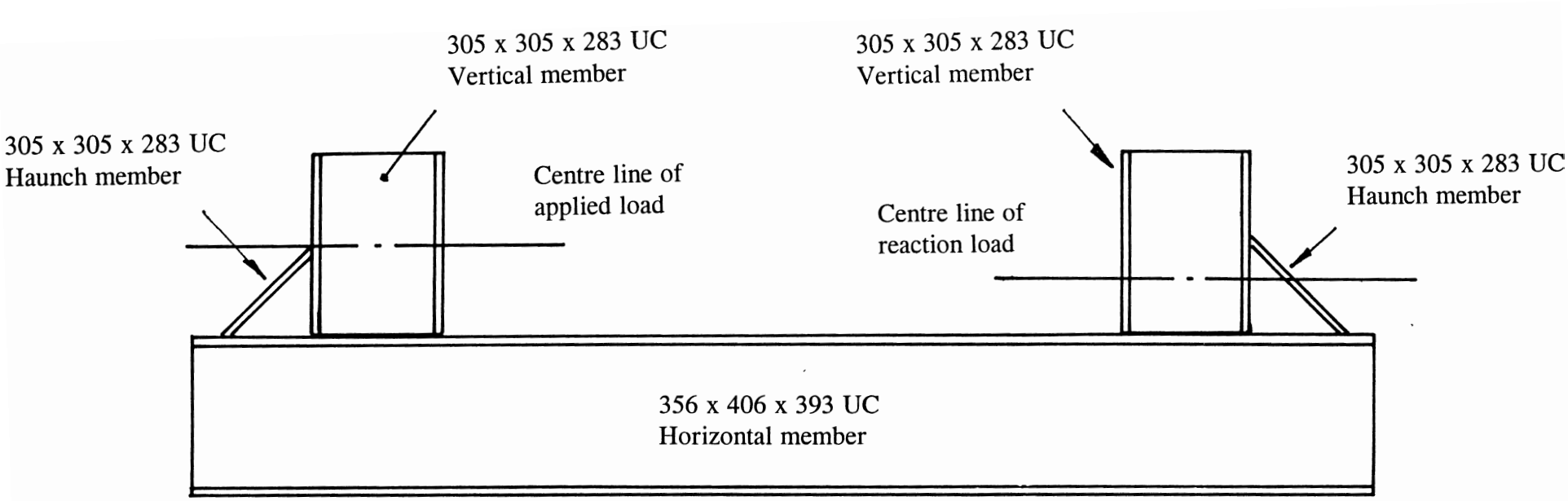

Figure 3.1 Test rig initially analysed

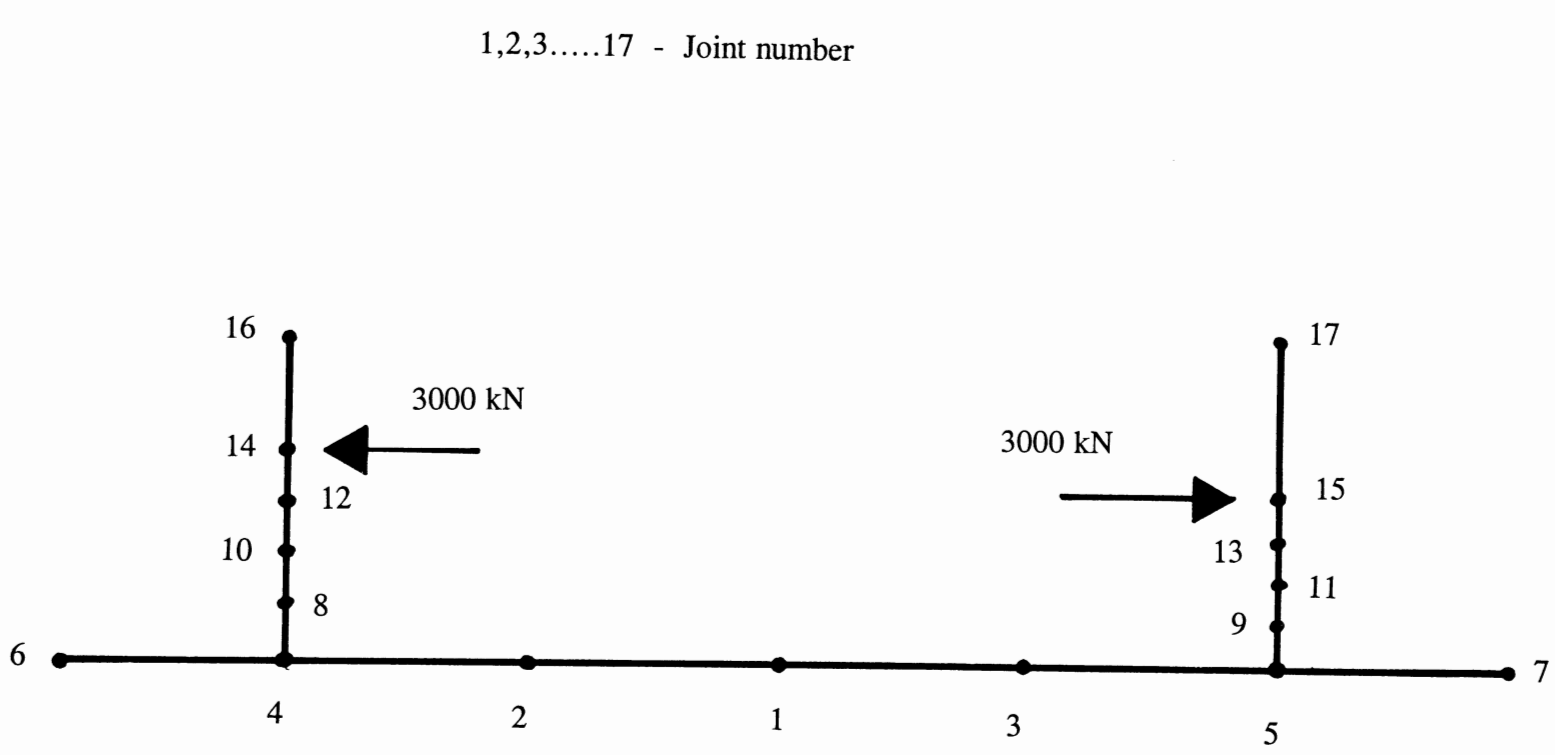

Note: For details of joint deflections, moments and stresses refer to Table 3.1 in section

Figure 3.2 Skeletal frame of the test rig analysed

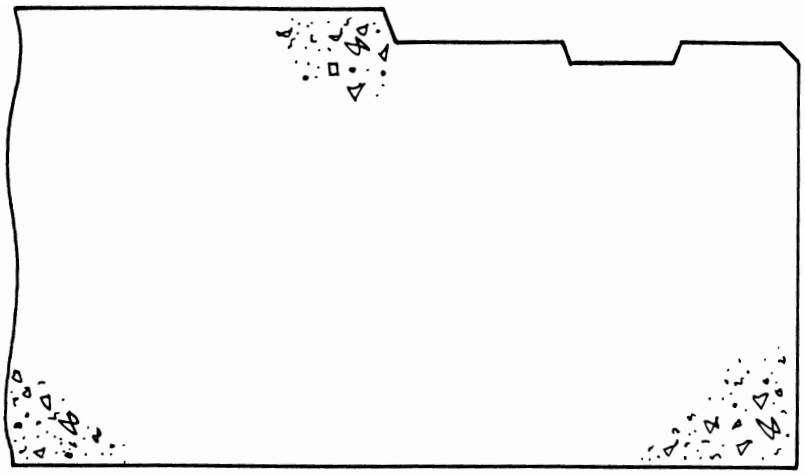

Figure 4.1 Standard ARC pipe (DN600) spigot detail

Note: Modification 1 includes 3° chamfer only
Modification 2 includes localised reinf't only
Modification 3 includes 3° chamfer + Local reinf't

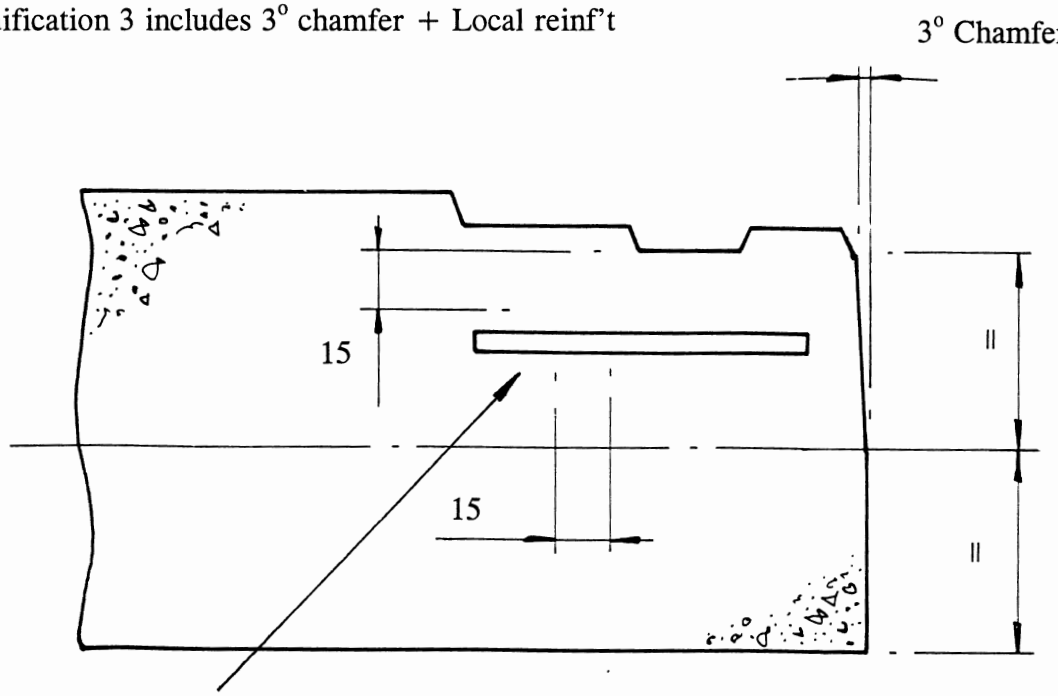

Figure 4.2 Modifications to ARC pipe (DN600) spigot detail

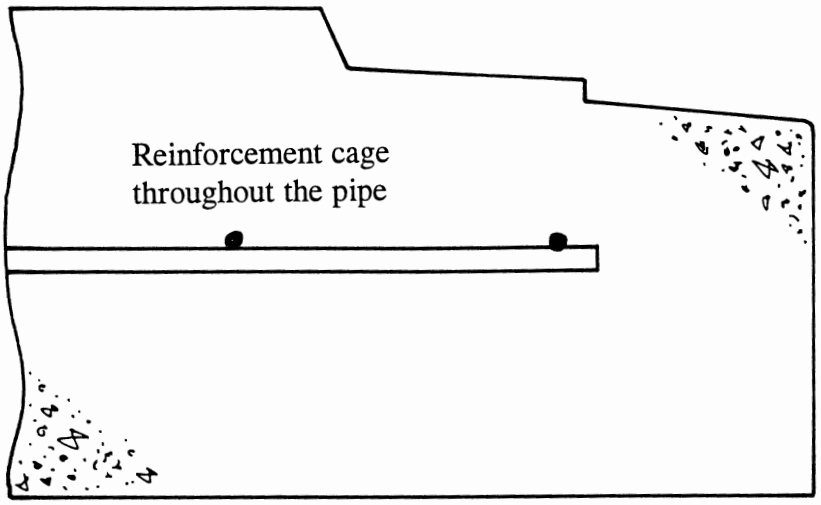

Figure 4.3 Standard Stanton Bonna pipe (DN600) spigot detail

Note: Modification 1 includes 2° chamfer only
Modification 2 includes localised reinf't only
Modification 3 includes 2° chamfer + Local reinf't

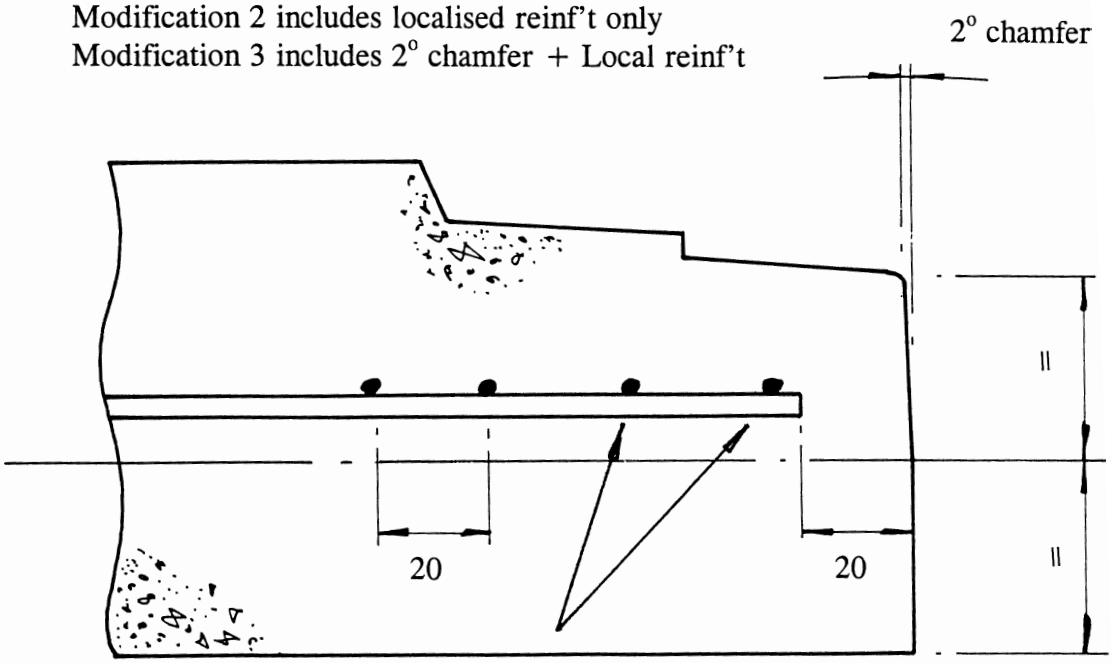

Longitudinal bars in standard cage extended and
the spacing of the last 4 hooped bars closed up

Figure 4.4 Modifications to Stanton Bonna pipe (DN600) spigot detail

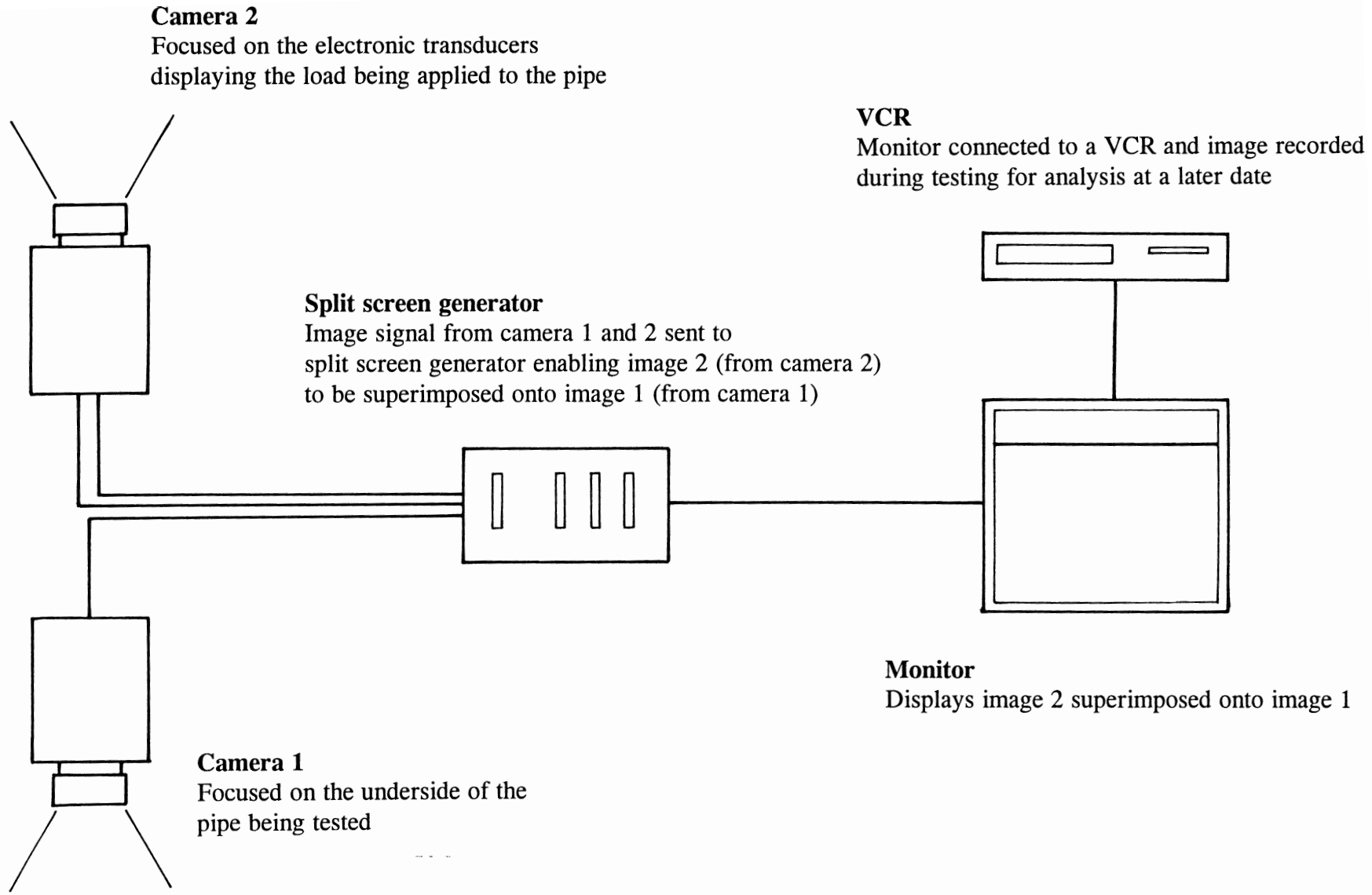

Figure 5.1 Schematic representation of data logging equipment

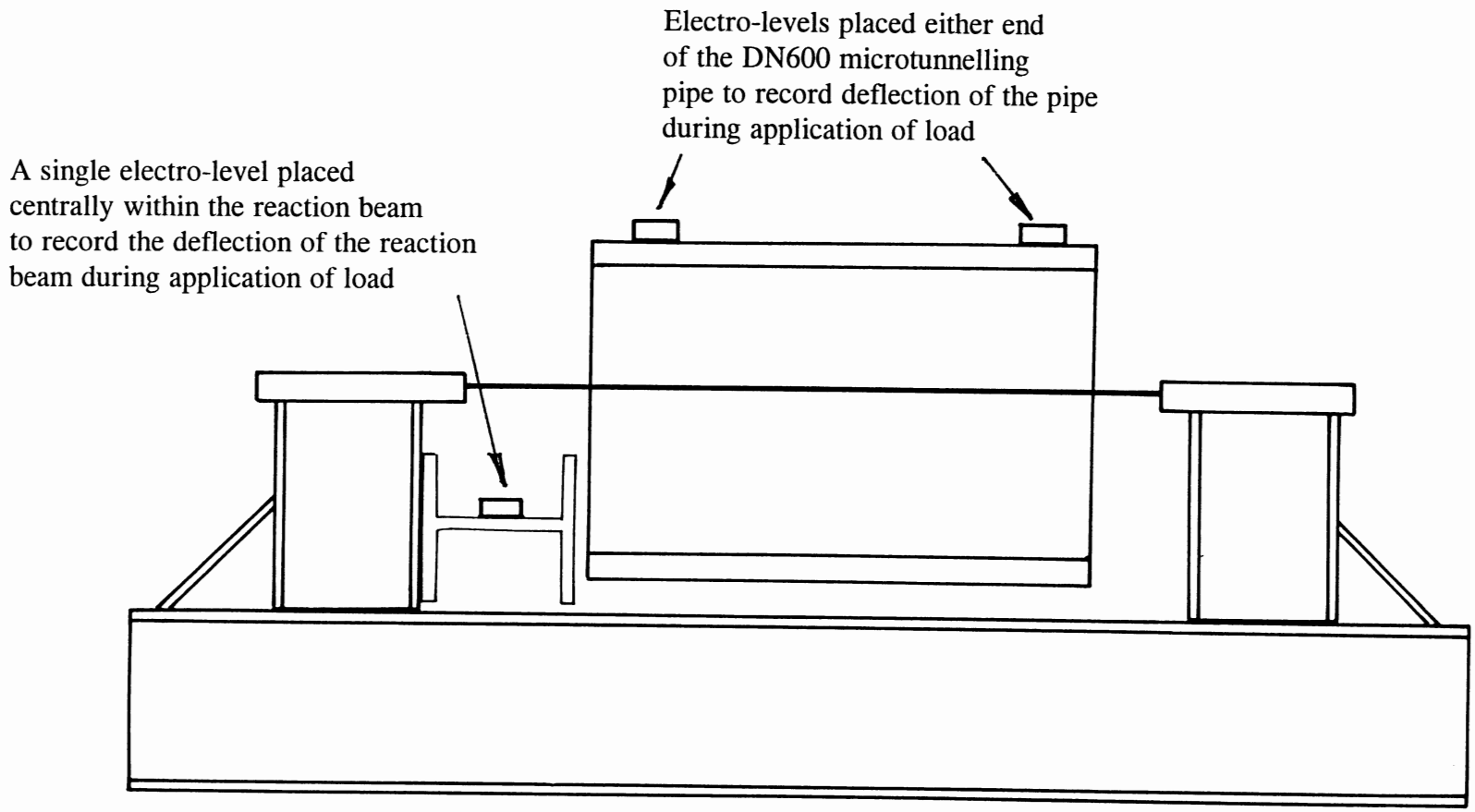

Figure 5.2 Location of electro-levels on the test rig and pipe

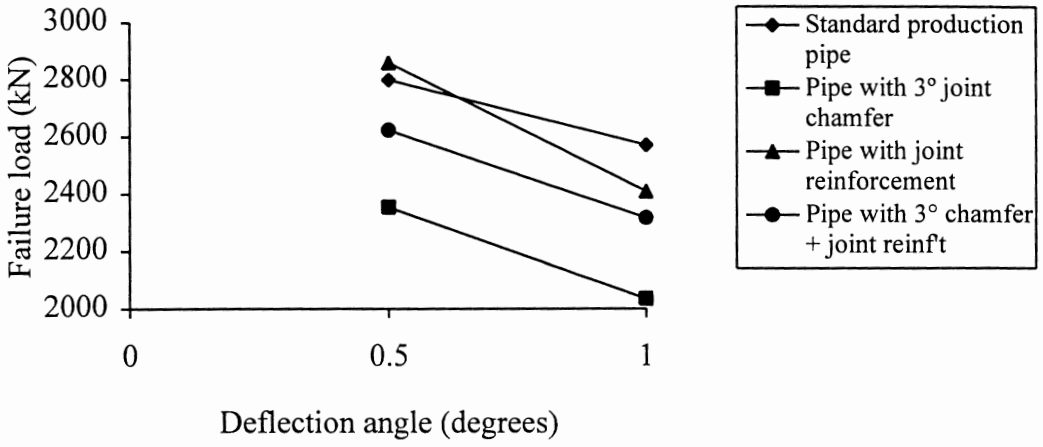

Figure 7.1 Effect of deflection angle on the failure load of ARC pipes.

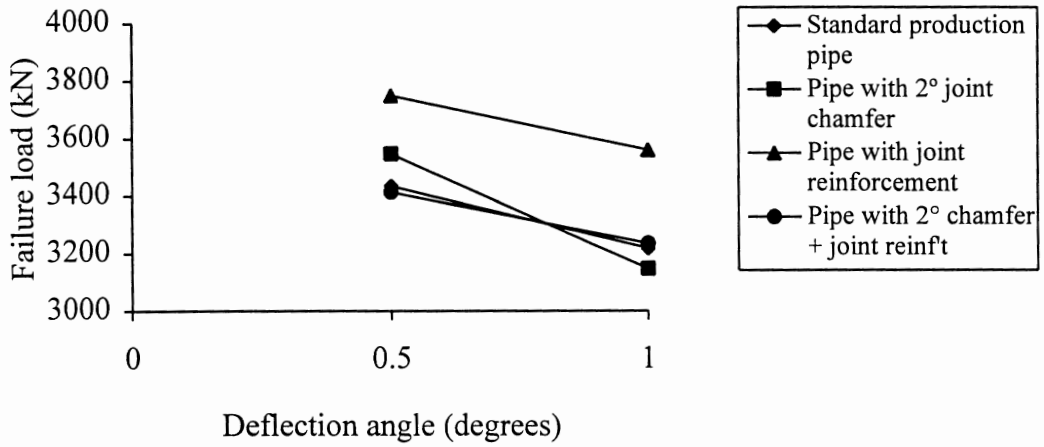

Figure 7.2 Effect of deflection angle on the failure load of Stanton Bonna pipes.

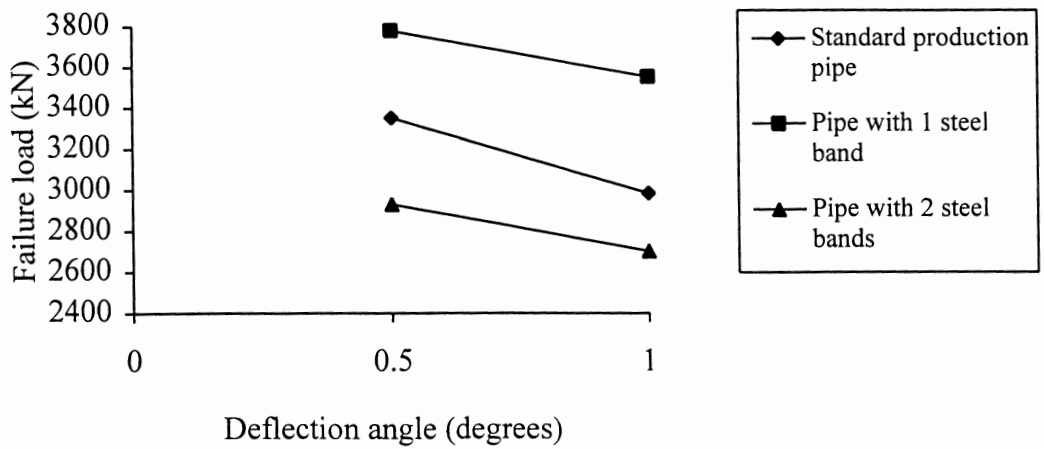

Figure 7.3 Effect of deflection angle on the failure load of Hepworth pipes.

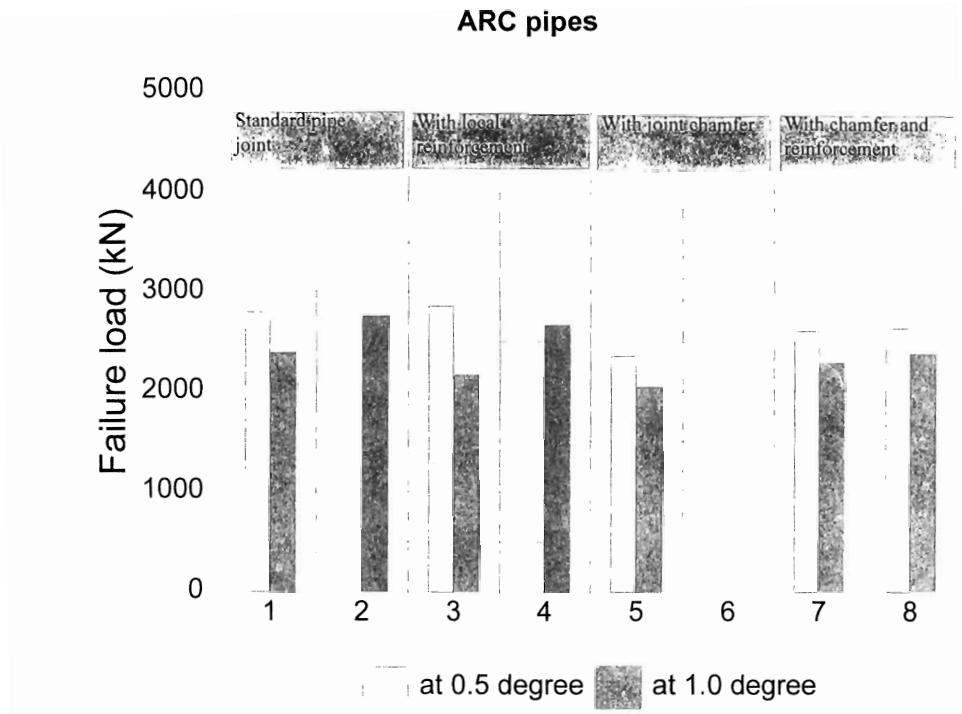

Figure 7.4 ARC pipe results

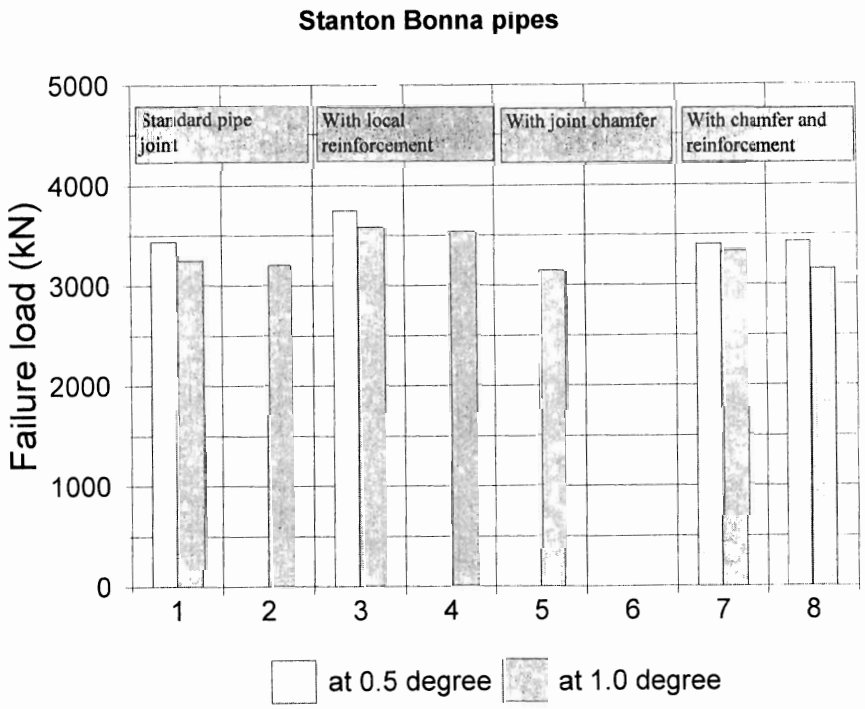

Figure 7.5 Stanton Bonna pipe results

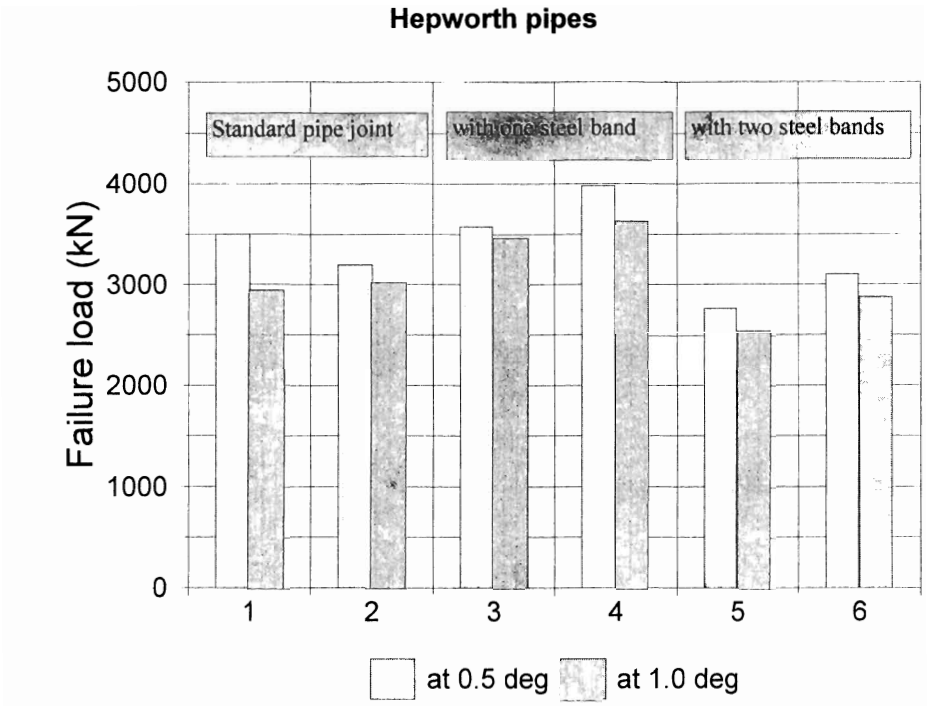

Figure 7.6 Hepworth pipe results

APPENDIX A

General Arrangements and details of test rig and pipe platform

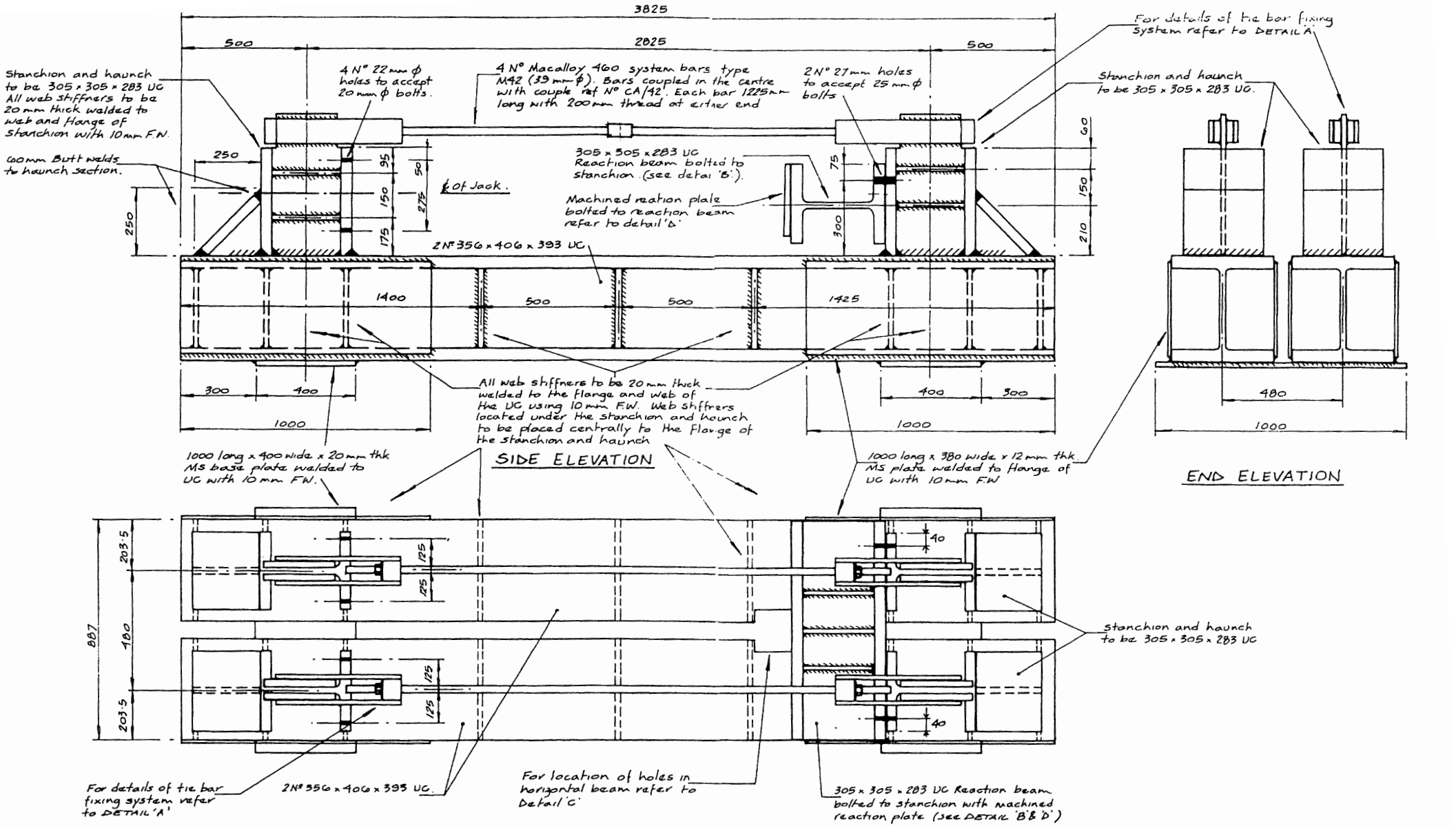

PLAN

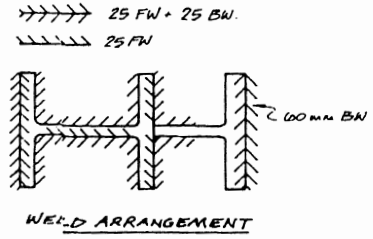

WELD ARRANGEMENT

NOTES:

1. WELDING OF BEAM TO STANCHION: Welding of 305 x 305 UC to 356 x 406 UC to comprise of 25mm Fillet welds and 25mm Fillet and Butt welds to all webs and flanges unless noted other wise (see sketch.)
2. REACTION BEAM: Reaction beam to be machined on both flanges to ensure a level surface is achieved
3. STANCHION ACCEPTING REACTION BEAM: The flange of the stanchion accepting reaction beam to be machined to ensure level surface. Stanchion to be erected ensuring that a vertical angle to the main horiz. beam of 90° ± 0·05° is maintained.

TEST RIG FOR PIPE JACKING RESEARCH PROJECT

GENERAL ARRANGEMENT

DATE: DEC '96

DRG. No: 01

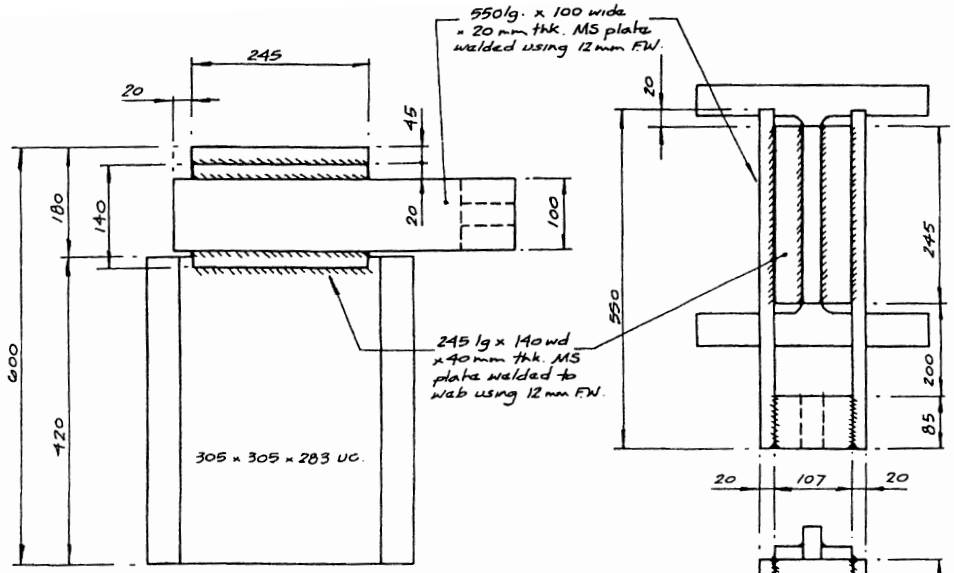

SIDE ELEVATION

PLAN AND END ELEVATION

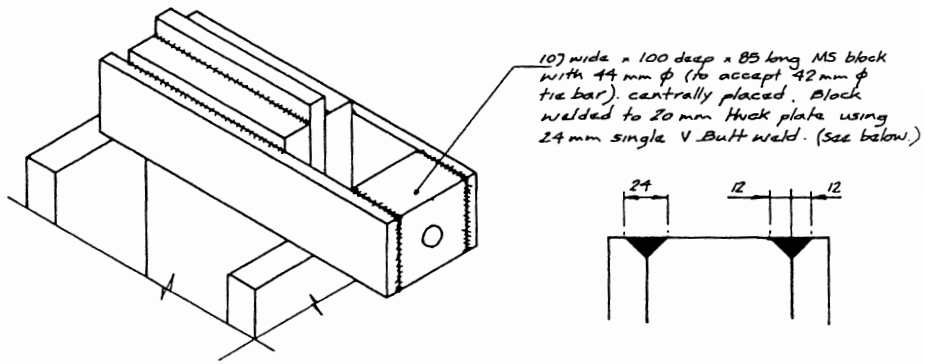

ISOMETRIC VIEW OF FIXING SYSTEM

DETAIL 'A'
(TIE BAR FIXING SYSTEM)

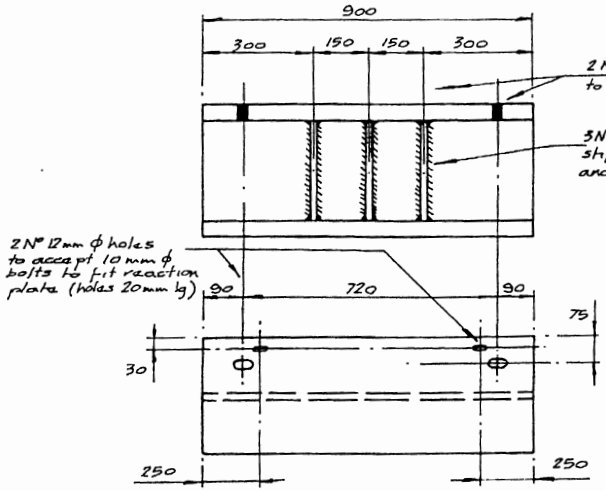

DETAIL 'B'
(REACTION BEAM)

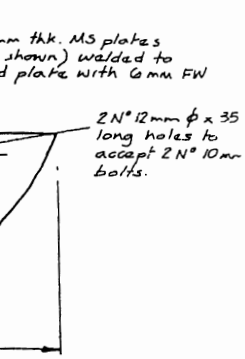

PLAN

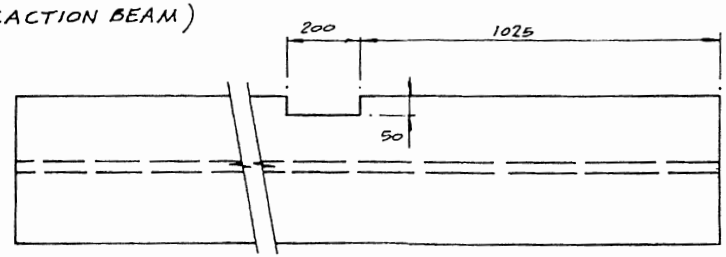

DETAIL 'C'
(POSITION OF HOLES IN HORIZONTAL BM.)

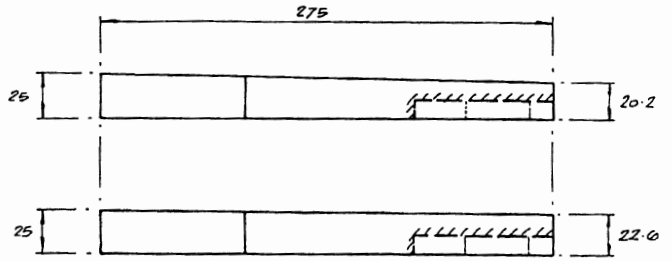

SIDE ELEVATIONS

DETAIL 'D'
(REACTION PLATE : 0·5° OR 1·0° CHAMFER.)

TEST RIG FOR PIPE JACKING RESEARCH PROJECT	
DATE: DEC '96	GENERAL DETAILS.
DRG. No.: 07	

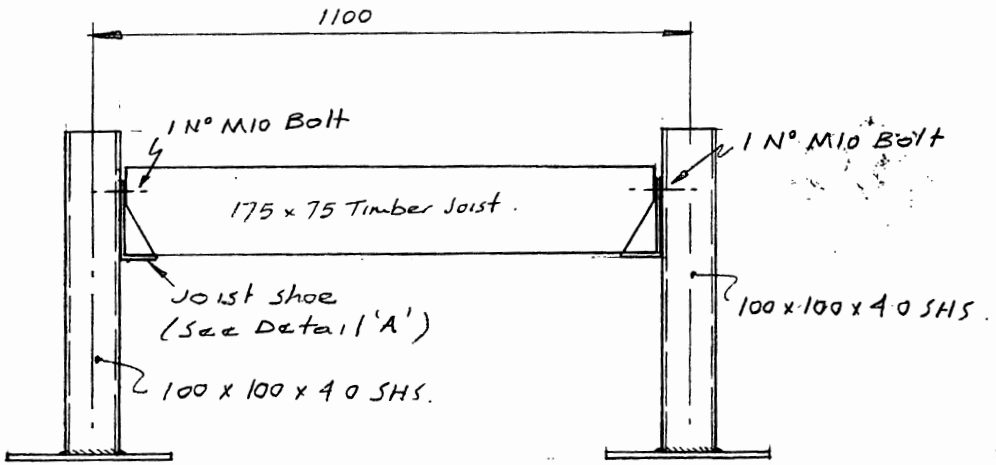

ELEVATION 'A'

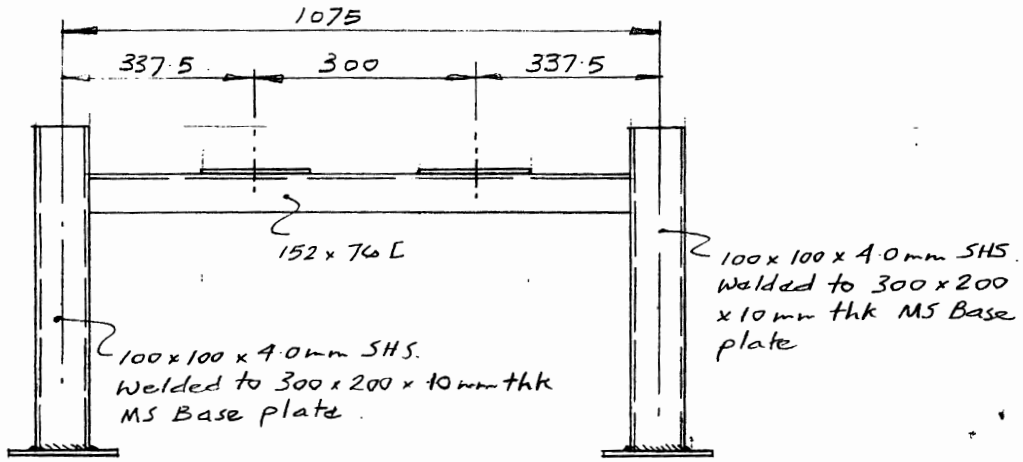

ELEVATION 'B'

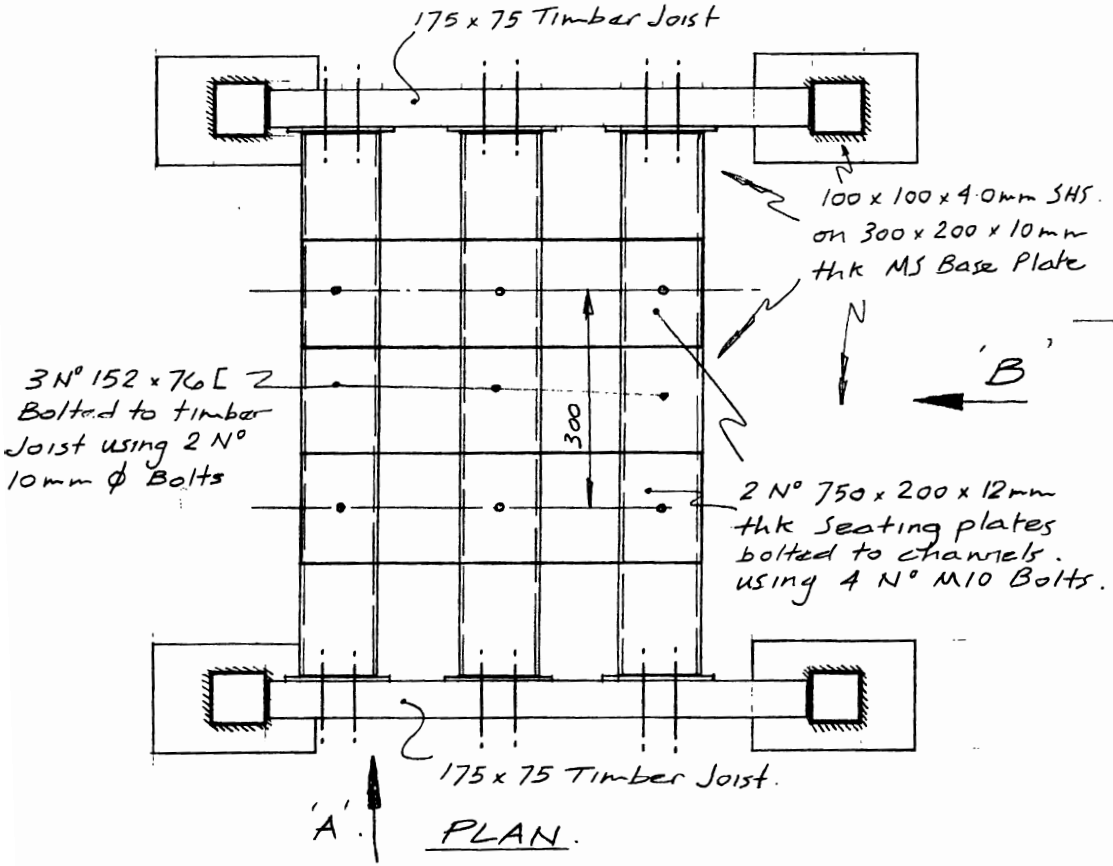

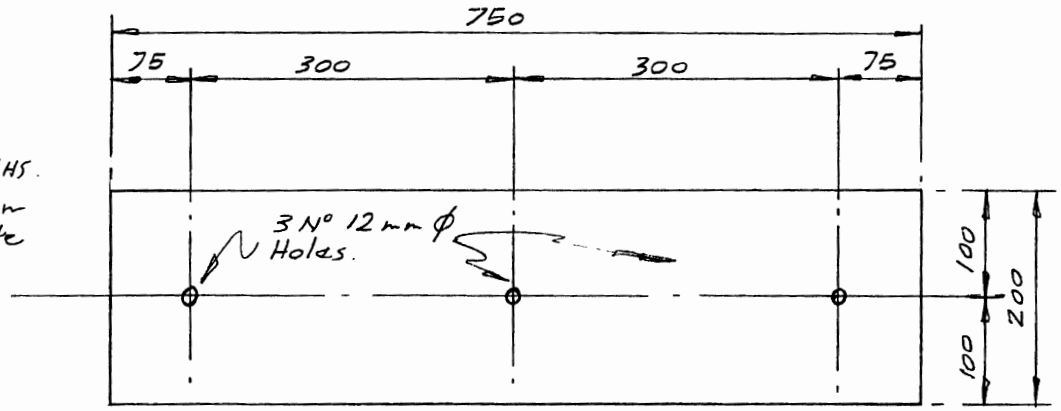

SEATING PLATE DETAIL

PIPE PLATFORM
GENERAL ARRANGEMENT.

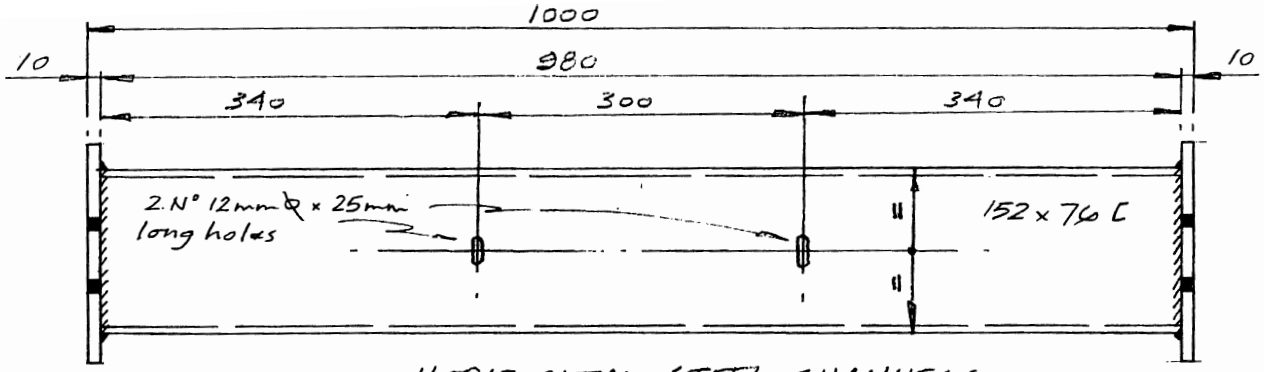

HORIZONTAL STEEL CHANNELS (3N°).

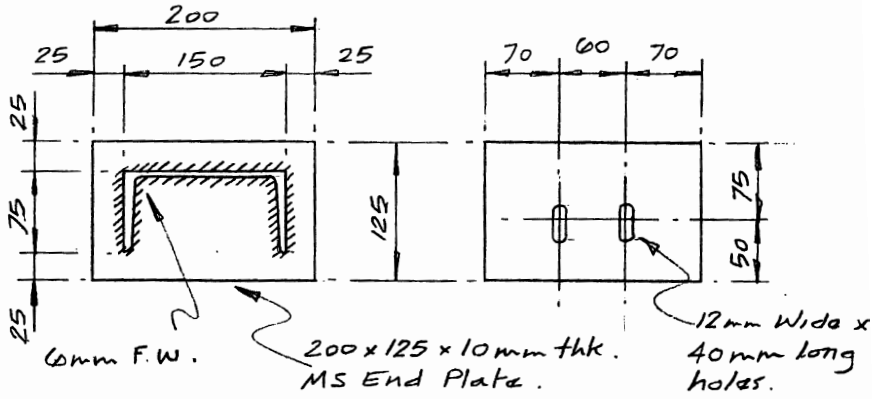

END PLATE DETAILS

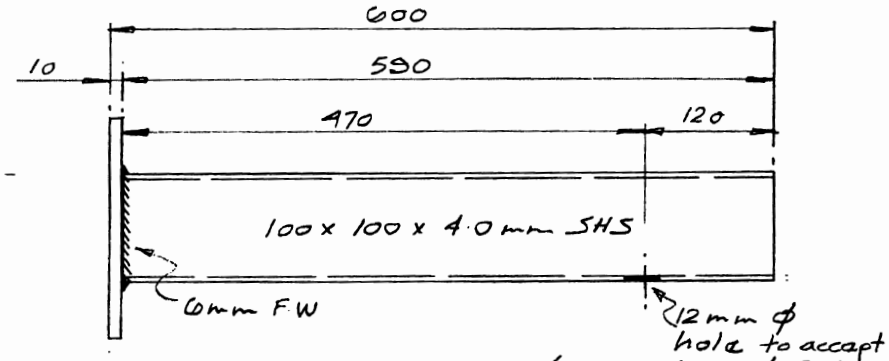

PLATFORM STANCHIONS (4N°)

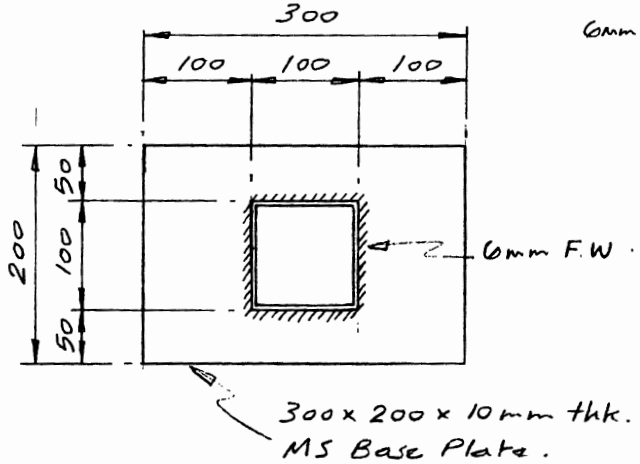

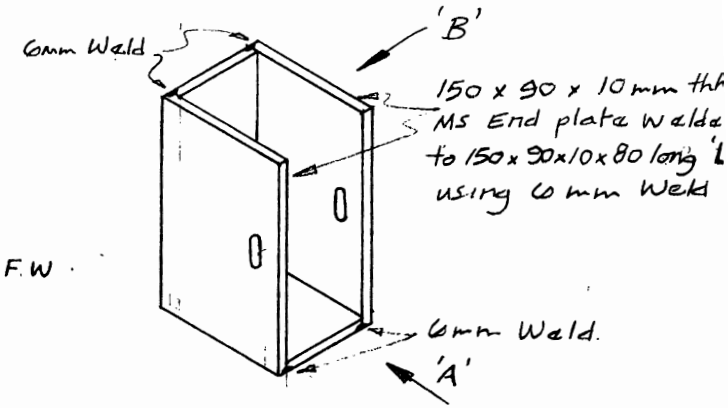

TIMBER JOIST SHOE (DETAIL 'A').

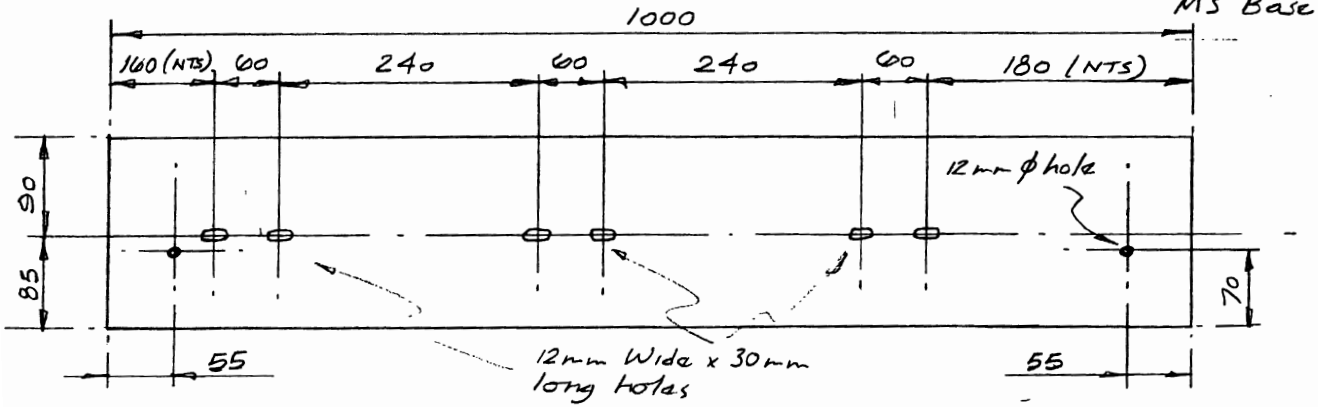

HORIZONTAL TIMBER JOIST (175 x 75)

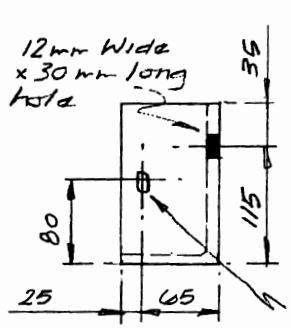

SIDE ELEVN (VIEW 'B')

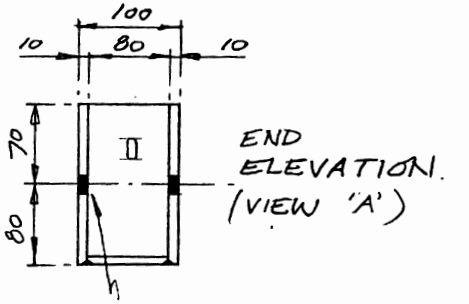

PIPE PLATFORM GENERAL DETAILS.

APPENDIX B

Electro-Level readings for ARC and Stanton Bonna pipes

Table B1 Electro level readings for ARC pipe 1 tested at 0.5°

Load (kN)	Electro level reading			Effect on β angle
	EL1	EL2	EL3	(EL1 - EL 2)/2 - EL3
500	0.048° (175)	0.051° (178)	0.041° (164)	0.0085°
1000	0.062° (221)	0.065° (227)	0.053° (200)	0.0105°
1500	0.077° (276)	0.077° (269)	0.058° (232)	0.019°
2000	0.093° (331)	0.096° (335)	0.063° (251)	0.032°
2500	0.106°(380)	0.109° (378)	0.067° (269)	0.040°

Note: Figures in parethesis are the actual electro level readings

Table B2 Electro level readings for ARC pipe 2 tested at 0.5°

Load (kN)	Electro level reading			Effect on β angle
	EL1	EL2	EL3	(EL1 - EL 2)/2 - EL3
500	0.040° (143)	0.040° (140)	0.031° (122)	0.009°
1000	0.059° (211)	0.051° (205)	0.044° (175)	0.011°
1500	0.074° (266)	0.065° (258)	0.053° (210)	0.017°
2000	0.087° (312)	0.077° (309)	0.059° (235)	0.023°
2500	0.099°(356)	0.087° (348)	0.065° (259)	0.028°

Note: Figures in parethesis are the actual electro level readings

Table B3 Electro level readings for ARC pipe 3 tested at 0.5°

Load (kN)	Electro level reading			Effect on β angle
	EL1	EL2	EL3	(EL1 - EL 2)/2 - EL3
500	0.055° (200)	0.058° (201)	0.047° (187)	0.0095°
1000	0.073° (261)	0.074° (256)	0.059° (235)	0.0145°
1500	0.087° (313)	0.089° (307)	0.066° (262)	0.022°
2000	0.100° (361)	0.103° (358)	0.069° (275)	0.0325°
2500	0.115°(412)	0.119° (412)	0.075° (298)	0.042°

Note: Figures in parethesis are the actual electro level readings

Table B4 Electro level readings ARC pipe 4 tested at 0.5°

Load (kN)	Electro level reading			Effect on β angle
	EL1	EL2	EL3	(EL1 - EL 2)/2 - EL3
500	0.037° (132)	0.037° (130)	0.030° (118)	0.007°
1000	0.052° (186)	0.052° (182)	0.040° (159)	0.012°
1500	0.061° (220)	0.062° (216)	0.046° (184)	0.015°
2000	0.073° (261)	0.075° (261)	0.050° (199)	0.024°
2500	0.082°(295)	0.084° (290)	0.052° (209)	0.031°

Note: Figures in parethesis are the actual electro level readings

Table B5 Electro level readings ARC pipe 5 tested at 0.5°

Load (kN)	Electro level reading			Effect on β angle
	EL1	EL2	EL3	(EL1 - EL 2)/2 - EL3
500	0.061° (218)	0.061° (214)	0.050° (199)	0.011°
1000	0.075° (270)	0.076° (265)	0.066° (230)	0.0095°
1500	0.088° (314)	0.089° (308)	0.075° (260)	0.0135°
2000	0.098° (352)	0.100° (348)	0.086° (300)	0.013°
2500	0.111°(397)	0.114° (397)	0.092° (320)	0.0205°

Note: Figures in parethesis are the actual electro level readings

Table B6 Electro level readings for ARC pipe 6 tested at 1.0°

Load (kN)	Electro level reading			Effect on β angle
	EL1	EL2	EL3	(EL1 - EL 2)/2 - EL3
500	0.071° (254)	0.072° (249)	0.058° (230)	0.0135°
1000	0.087° (311)	0.088° (305)	0.068° (273)	0.0195°
1500	0.103° (367)	0.104° (362)	0.078° (313)	0.0255°
2000	0.112° (404)	0.115° (399)	0.084° (335)	0.0295°

Note: Figures in parethesis are the actual electro level readings

Table B7 Electro level readings for ARC pipe 7 tested at 1.0°

Load (kN)	Electro level reading			Effect on β angle
	EL1	EL2	EL3	(EL1 - EL 2)/2 - EL3
500	0.032° (114)	0.032° (111)	0.024° (99)	0.0008°
1000	0.046° (165)	0.047° (163)	0.033° (132)	0.0135°
1500	0.055° (198)	0.056° (195)	0.040° (159)	0.0155°
2000	0.065° (231)	0.065° (227)	0.044° (178)	0.021°

Note: Figures in parethesis are the actual electro level readings

Table B8 Electro level readings ARC pipe 8 tested at 1.0°

Load (kN)	Electro level reading			Effect on β angle
	EL1	EL2	EL3	(EL1 - EL 2)/2 - EL3
500	0.043° (154)	0.043° (150)	0.032° (131)	0.011°
1000	0.061° (217)	0.062° (215)	0.046° (182)	0.0155°
1500	0.075° (269)	0.077° (268)	0.055° (220)	0.021°
2000	0.089° (317)	0.091° (314)	0.064° (255)	0.026°

Note: Figures in parethesis are the actual electro level readings

Table B9 Electro level readings for ARC pipe 9 tested at 1.0°

Load (kN)	Electro level reading			Effect on β angle
	EL1	EL2	EL3	(EL1 - EL 2)/2 - EL3
500	0.049° (176)	0.050° (174)	0.038° (150)	0.115°
1000	0.062° (223)	0.063° (219)	0.045° (179)	0.0175°
1500	0.075° (267)	0.076° (263)	0.051° (205)	0.0245°
2000	0.090° (321)	0.092° (320)	0.058° (230)	0.033°
2500	0.103°(367)	0.106° (367)	0.062° (249)	0.0425°

Note: Figures in parethesis are the actual electro level readings

Table B10 Electro level readings ARC pipe 10 tested at 1.0°

Load (kN)	Electro level reading			Effect on β angle
	EL1	EL2	EL3	(EL1 - EL 2)/2 - EL3
500	0.046° (163)	0.046° (160)	0.035° (138)	0.010°
1000	0.060° (216)	0.061° (213)	0.043° (172)	0.0165°
1500	0.072° (257)	0.074° (256)	0.048° (190)	0.025°
2000	0.084° (301)	0.087° (302)	0.053° (212)	0.0325°

Note: Figures in parethesis are the actual electro level readings

Table B11 Electro level readings for ARC pipe 11 tested at 1.0°

Load (kN)	Electro level reading			Effect on β angle
	EL1	EL2	EL3	(EL1 - EL 2)/2 - EL3
500	0.034° (123)	0.034° (118)	0.025° (98)	0.009°
1000	0.048° (171)	0.048° (167)	0.034° (135)	0.014°
1500	0.061° (219)	0.062° (216)	0.042° (167)	0.0195°
2000	0.072° (258)	0.074° (258)	0.047° (187)	0.026°

Note: Figures in parethesis are the actual electro level readings

Table B12 Electro level readings for ARC pipe 12 tested at 1.0°

Load (kN)	Electro level reading			Effect on β angle
	EL1	EL2	EL3	(EL1 - EL 2)/2 - EL3
500	0.053° (189)	0.054° (188)	0.041° (164)	0.0125°
1000	0.068° (243)	0.069° (241)	0.051° (203)	0.0175°
1500	0.082° (292)	0.084° (291)	0.059° (235)	0.024°
2000	0.090° (323)	0.093° (323)	0.064° (255)	0.0275°

Note: Figures in parethesis are the actual electro level readings

Table B13 Electro level readings for Stanton Bonna pipe 1 tested at 0.5°

Load (kN)	Electro level reading			Effect on β angle
	EL1	EL2	EL3	(EL1 - EL 2)/2 - EL3
500	0.040° (142)	0.041° (143)	0.030° (121)	0.00105°
1000	0.053° (190)	0.055° (191)	0.040° (159)	0.014°
1500	0.067° (239)	0.069° (239)	0.049° (196)	0.019°
2000	0.080° (287)	0.083° (286)	0.058° (231)	0.0235°
2500	0.093°(331)	0.095° (328)	0.064° (256)	0.030°
3000	0.101° (362)	0.104° (359)	0.067° (267)	0.0355°

Note: Figures in parethesis are the actual electro level readings

Table B14 Electro level readings for Stanton Bonna pipe 2 tested at 0.5°

Load (kN)	Electro level reading			Effect on β angle
	EL1	EL2	EL3	(EL1 - EL 2)/2 - EL3
500	0.022° (78)	0.022° (76)	0.015° (58)	0.007°
1000	0.037° (134)	0.038° (132)	0.024° (97)	0.0135°
1500	0.050° (178)	0.051° (178)	0.033° (130)	0.0175°
2000	0.062° (222)	0.063° (219)	0.041° (165)	0.0215°
2500	0.074°(263)	0.075° (260)	0.045° (182)	0.0295°
3000	0.084° (301)	0.086° (298)	0.051° (202)	0.034°

Note: Figures in parethesis are the actual electro level readings

Table B15 Electro level readings for Stanton Bonna pipe 3 tested at 0.5°

Load (kN)	Electro level reading			Effect on β angle
	EL1	EL2	EL3	(EL1 - EL 2)/2 - EL3
500	0.035° (126)	0.035° (123)	0.026° (104)	0.009°
1000	0.048° (173)	0.049° (170)	0.034° (137)	0.0145°
1500	0.062° (223)	0.064° (223)	0.041° (165)	0.022°
2000	0.074° (264)	0.076° (263)	0.047° (189)	0.028°
2500	0.083°(297)	0.085° (295)	0.053° (211)	0.031°
3000	0.092° (330)	0.094°(325)	0.056° (225)	0.037°

Note: Figures in parethesis are the actual electro level readings

Table B16 Electro level readings for Stanton Bonna pipe 4 tested at 0.5°

Load (kN)	Electro level reading			Effect on β angle
	EL1	EL2	EL3	(EL1 - EL 2)/2 - EL3
500	0.061° (218)	0.062° (214)	0.048° (192)	0.0135°
1000	0.074° (265)	0.076° (262)	0.057° (229)	0.018°
1500	0.087° (313)	0.090° (312)	0.066° (265)	0.0225°
2000	0.099° (356)	0.102° (356)	0.074° (297)	0.031°
2500	0.110°(393)	0.113° (393)	0.081° (323)	0.034°
3000	0.119° (427)	0.123° (428)	0.084° (335)	0.037°

Note: Figures in parethesis are the actual electro level readings

Table B17 Electro level readings for Stanton Bonna pipe 5 tested at 0.5°

Load (kN)	Electro level reading			Effect on β angle
	EL1	EL2	EL3	(EL1 - EL 2)/2 - EL3
500	0.053° (191)	0.054° (188)	0.042° (169)	0.0115°
1000	0.067° (241)	0.069° (240)	0.051° (205)	0.017°
1500	0.080° (286)	0.082° (284)	0.059° (237)	0.022°
2000	0.090° (323)	0.093° (321)	0.066° (265)	0.0255°
2500	0.100°(358)	0.102° (355)	0.070° (281)	0.031°
3000	0.108° (387)	0.111(384)	0.073° (290)	0.0365°

Note: Figures in parethesis are the actual electro level readings

Table B18 Electro level readings for Stanton Bonna pipe 6 tested at 1.0°

Load (kN)	Electro level reading			Effect on β angle
	EL1	EL2	EL3	(EL1 - EL 2)/2 - EL3
500	0.054° (192)	0.055° (192)	0.044° (176)	0.0105°
1000	0.069° (240)	0.069° (239)	0.053° (212)	0.016°
1500	0.083° (289)	0.083° (287)	0.060° (238)	0.023°
2000	0.097° (335)	0.096° (332)	0.066° (265)	0.0305°
2500	0.107° (371)	0.106° (368)	0.070°(281)	0.0365°
3000	0.115° (398)	0.115° (399)	0.073°(293)	0.042°

Note: Figures in parethesis are the actual electro level readings

Table B19 Electro level readings for Stanton Bonna pipe 7 tested at 1.0°

Load (kN)	Electro level reading			Effect on β angle
	EL1	EL2	EL3	(EL1 - EL 2)/2 - EL3
500	0.033° (117)	0.033° (115)	0.026° (104)	0.007°
1000	0.045° (161)	0.046° (160)	0.035° (139)	0.0105°
1500	0.057° (203)	0.057° (199)	0.041° (164)	0.016°
2000	0.070° (251)	0.071° (248)	0.047° (187)	0.0235°
2500	0.081° (289)	0.082° (285)	0.055° (220)	0.0265°
3000	0.091° (324)	0.093° (322)	0.061° (245)	0.031°

Note: Figures in parethesis are the actual electro level readings

Table B20 Electro level readings for Stanton Bonna pipe 8 tested at 1.0°

Load (kN)	Electro level reading			Effect on β angle
	EL1	EL2	EL3	(EL1 - EL 2)/2 - EL3
500	0.040° (143)	0.041° (142)	0.033° (131)	0.0075°
1000	0.054° (194)	0.055° (192)	0.042° (168)	0.0125°
1500	0.067° (239)	0.068° (239)	0.050° (200)	0.0175°
2000	0.079° (284)	0.081° (282)	0.056° (224)	0.024°
2500	0.090° (323)	0.092° (321)	0.062° (248)	0.029°
3000	0.100° (358)	0.103° (356)	0.065° (261)	0.0365°

Note: Figures in parethesis are the actual electro level readings

Table B21 Electro level readings for Stanton Bonna pipe 9 tested at 1.0°

Load (kN)	Electro level reading			Effect on β angle
	EL1	EL2	EL3	(EL1 - EL 2)/2 - EL3
500	0.025° (91)	0.027° (92)	0.022° (86)	0.004°
1000	0.041° (145)	0.041° (143)	0.030° (121)	0.011°
1500	0.055° (197)	0.056° (195)	0.040° (162)	0.0155°
2000	0.067° (239)	0.068° (236)	0.045° (181)	0.0225°
2500	0.076°(272)	0.078° (271)	0.050° (199)	0.027°
3000	0.085° (304)	0.088° (305)	0.053° (213)	0.0335°

Note: Figures in parethesis are the actual electro level readings

Table B22 Electro level readings for Stanton Bonna pipe 10 tested at 1.0°

Load (kN)	Electro level reading			Effect on β angle
	EL1	EL2	EL3	(EL1 - EL 2)/2 - EL3
500	0.032° (111)	0.031° (109)	0.024° (98)	0.0075°
1000	0.045° (156)	0.045° (155)	0.033° (131)	0.012°
1500	0.057° (199)	0.057° (197)	0.040° (159)	0.017°
2000	0.069° (241)	0.069° (241)	0.046° (184)	0.025°
2500	0.079° (275)	0.079° (273)	0.050° (201)	0.029°
3000	0.089°(310)	0.089° (308)	0.052° (211)	0.037°

Note: Figures in parethesis are the actual electro level readings

Table B23 Electro level readings for Stanton Bonna pipe 11 tested at 1.0°

Load (kN)	Electro level reading			Effect on β angle
	EL1	EL2	EL3	(EL1 - EL 2)/2 - EL3
500	0.046° (163)	0.046° (160)	0.037° (149)	0.009°
1000	0.059° (212)	0.060° (209)	0.046° (185)	0.0135°
1500	0.071° (254)	0.073° (253)	0.054° (216)	0.018°
2000	0.084° (300)	0.086° (298)	0.060° (241)	0.025°
2500	0.095° (341)	0.097° (338)	0.065° (258)	0.031°
3000	0.106° (379)	0.109° (377)	0.069° (277)	0.0385°

Note: Figures in parethesis are the actual electro level readings

Table B24 Electro level readings for Stanton Bonna pipe 12 tested at 1.0°

Load (kN)	Electro level reading			Effect on β angle
	EL1	EL2	EL3	(EL1 - EL 2)/2 - EL3
500	0.040° (143)	0.041° (142)	0.032° (129)	0.0085°
1000	0.053° (190)	0.054° (187)	0.042° (169)	0.0115°
1500	0.065° (232)	0.067° (231)	0.049° (197)	0.017°
2000	0.075° (269)	0.077° (267)	0.057° (226)	0.019°
2500	0.087° (311)	0.089° (310)	0.063° (252)	0.025°
3000	0.097° (346)	0.099° (345)	0.066° (265)	0.032°

Note: Figures in parethesis are the actual electro level readings

APPENDIX C

Video sequences of pipe failures

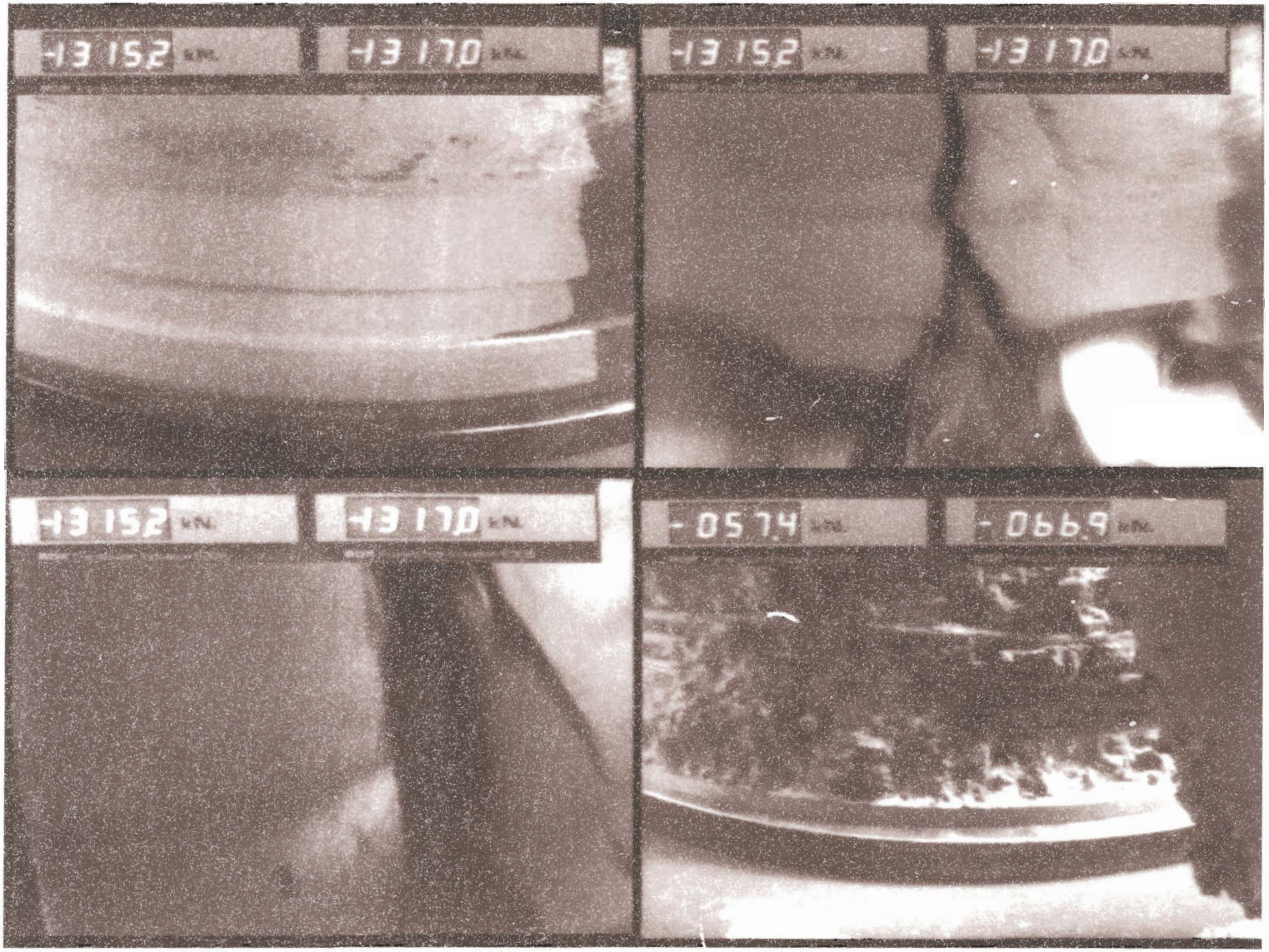
+3 152 KNL
+3 170 KNL
+3 152 KNL
+3 170 KNL
+3 152 KNL
+3 170 KNL
- 057.4 KNL
- 066.9 KNL

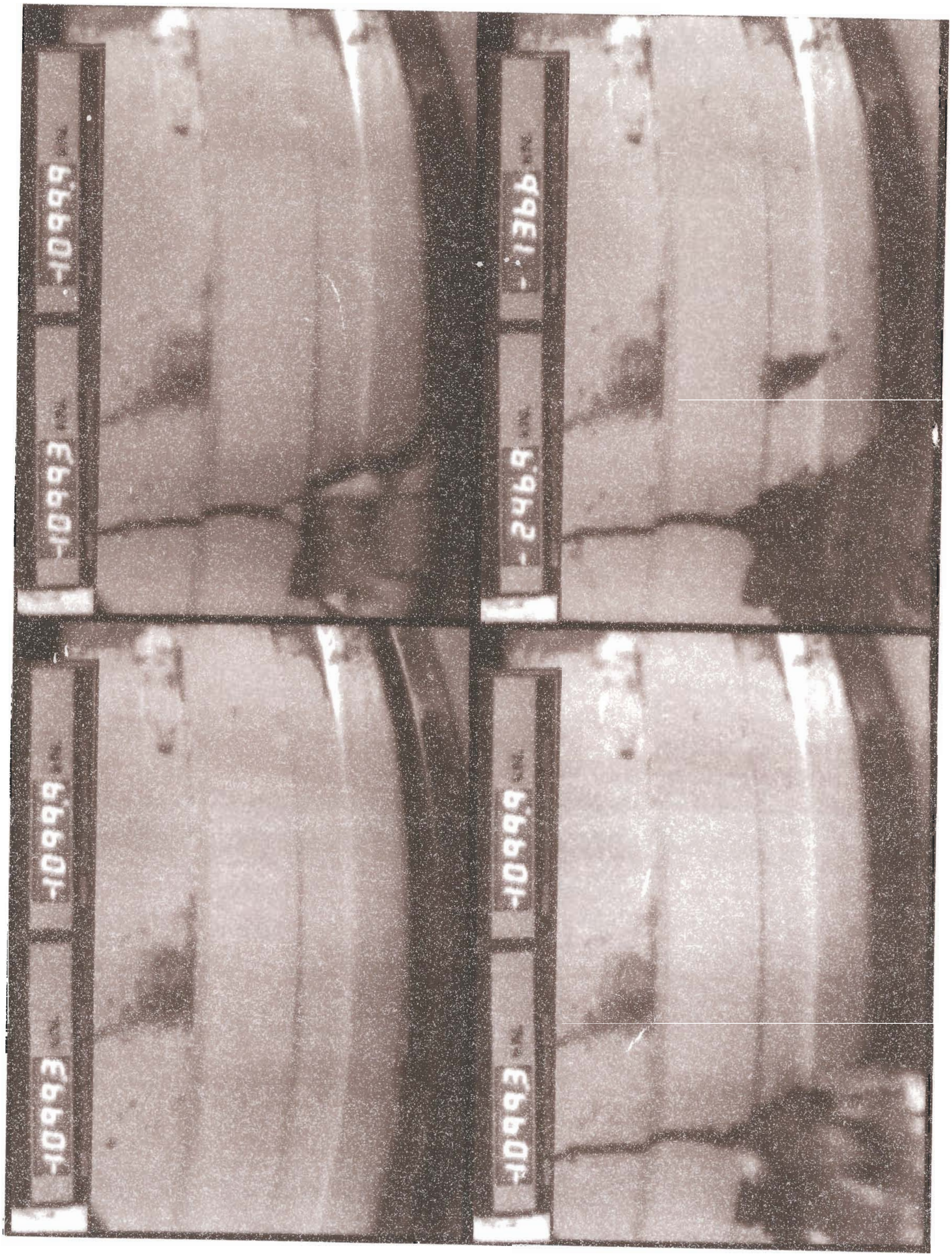

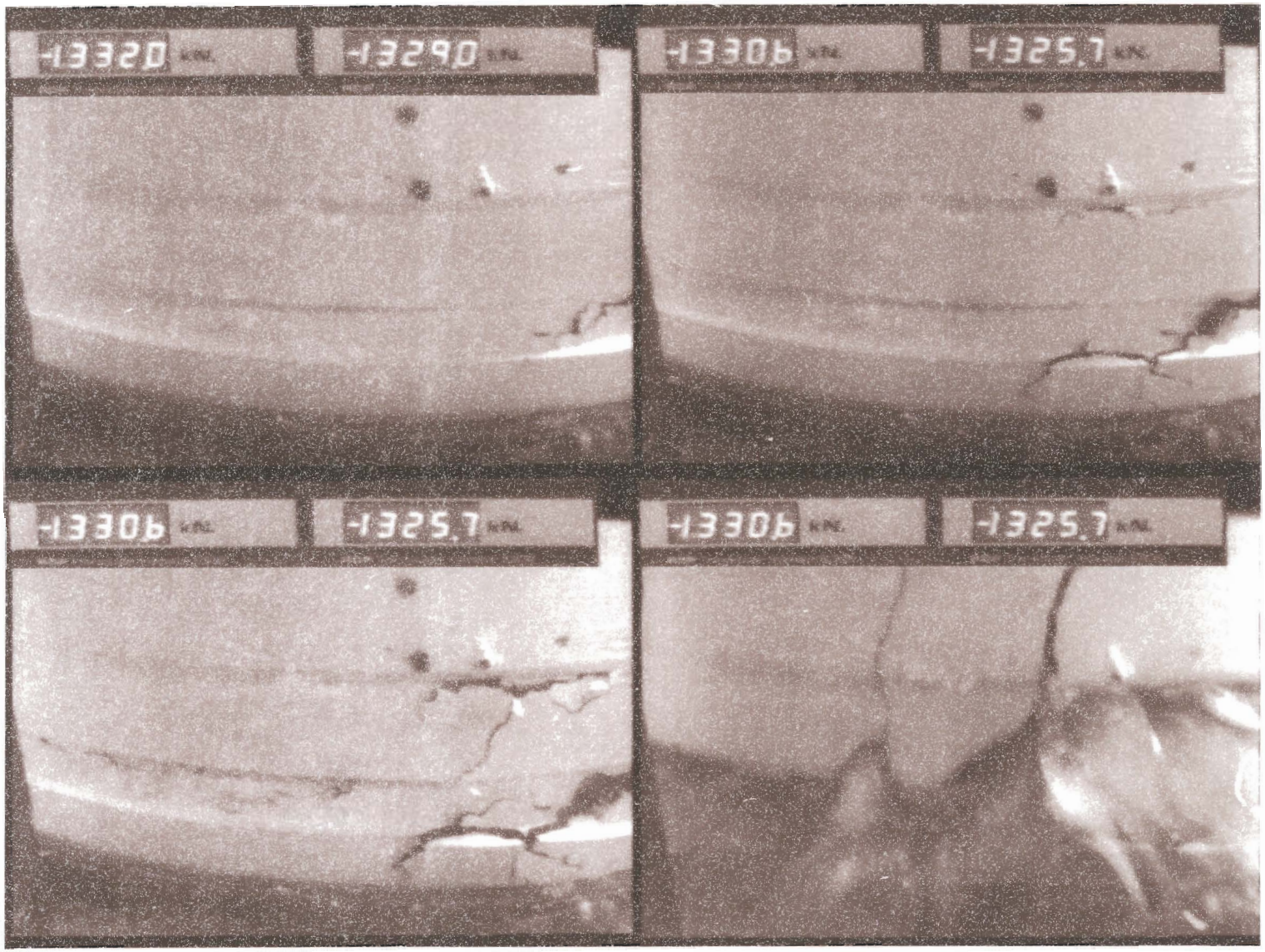
-1332.0 kN
-1329.0 kN
-1330.6 kN
-1325.7 kN
-1330.6 kN
-1325.7 kN
-1330.6 kN
-1325.7 kN

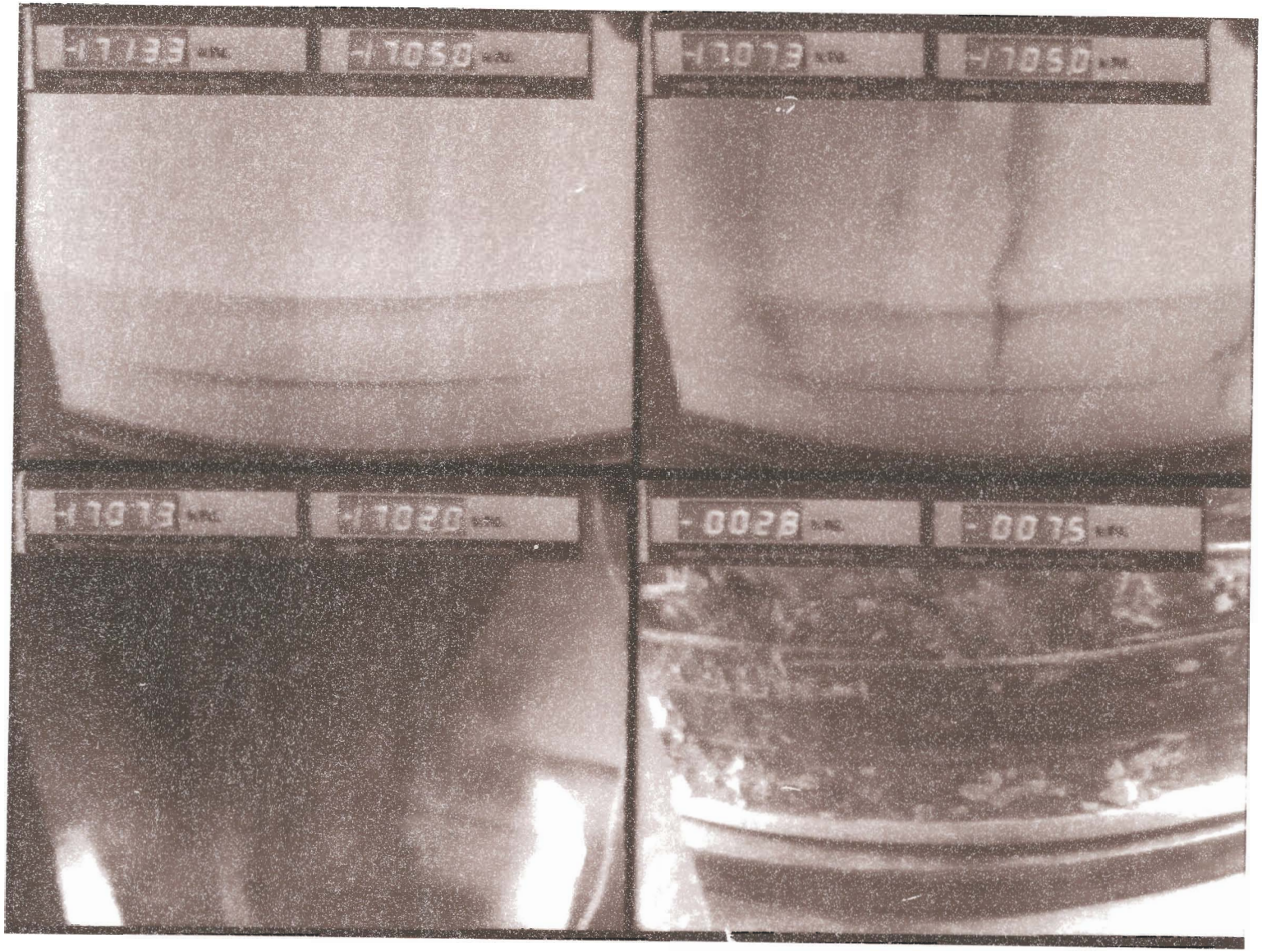
H 7133 M/KL
H 7050 M/KL
H 7073 M/KL
H 7050 M/KL
H 7073 M/KL
H 7020 M/KL
- 0028 M/KL
- 0075 M/KL

14:40
14:42
14:45
14:48
14:49
14:51
14:53
14:54

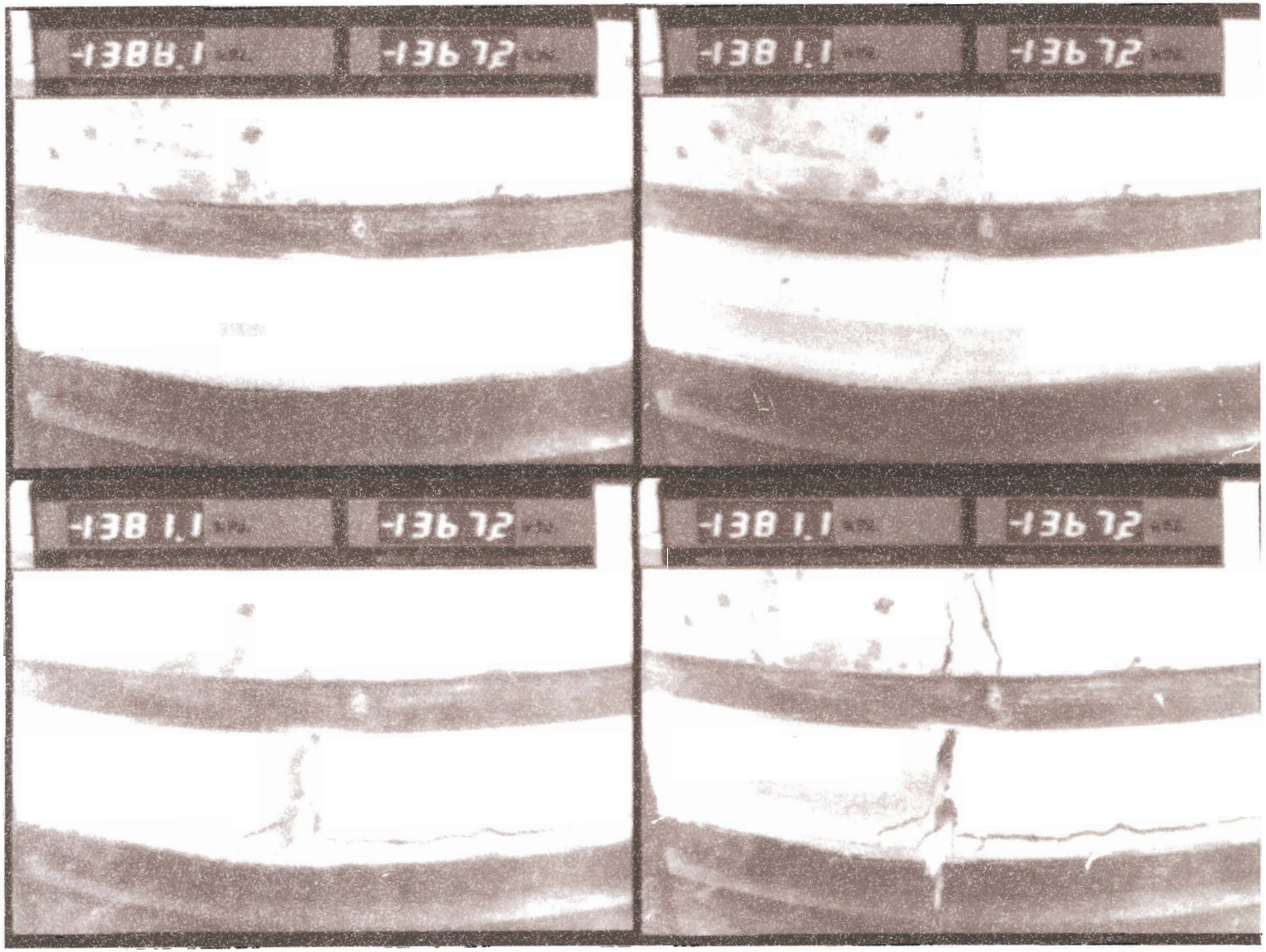
-1381.1
-1367.2
-1381.1
-1367.2
-1381.1
-1367.2
-1381.1
-1367.2

ARC pipe 3 (standard pipe + joint reinforcement tested at 0.5°)

ARC pipe 10 (standard pipe + joint reinforcement tested at 1.0°)

ARC pipe 11 (standard pipe + 3° chamfer + joint reinf't tested at 1.0°)

Stanton Bonna pipe 11 (standard pipe + 2° chamfer + joint reinf't tested at 1.0°)

Stanton Bonna pipe 13 (standard pipe unreinforced)

Hepworth pipe 5 (standard pipe with 2 steel bands tested at 0.5^{o})

APPENDIX D

Photographic catalogue of pipe failures

Plate 3.1 Test rig and pipe platform for DN600 microtunnelling pipes

Plate 4.1 Cage of joint reinforcement in ARC DN600 pipe mould.

Plate 4.2 Modifications incorporated at the spigot joint of Hepworth pipes.

Plate D1 Pipe 2: Standard production with 3° chamfer (0.5° deflection)

Plate D2 Pipe 3: Standard pipe with joint reinforcement (0.5° deflection)

Plate D3 Pipe 4: Standard pipe with 3° and joint reinf't chamfer (0.5° deflection)

Plate D4 Pipe 5: Standard pipe with 3° chamfer and joint reinf't (0.5° deflection)

Plate D5 Pipe 6: Standard pipe (1.0° deflection)

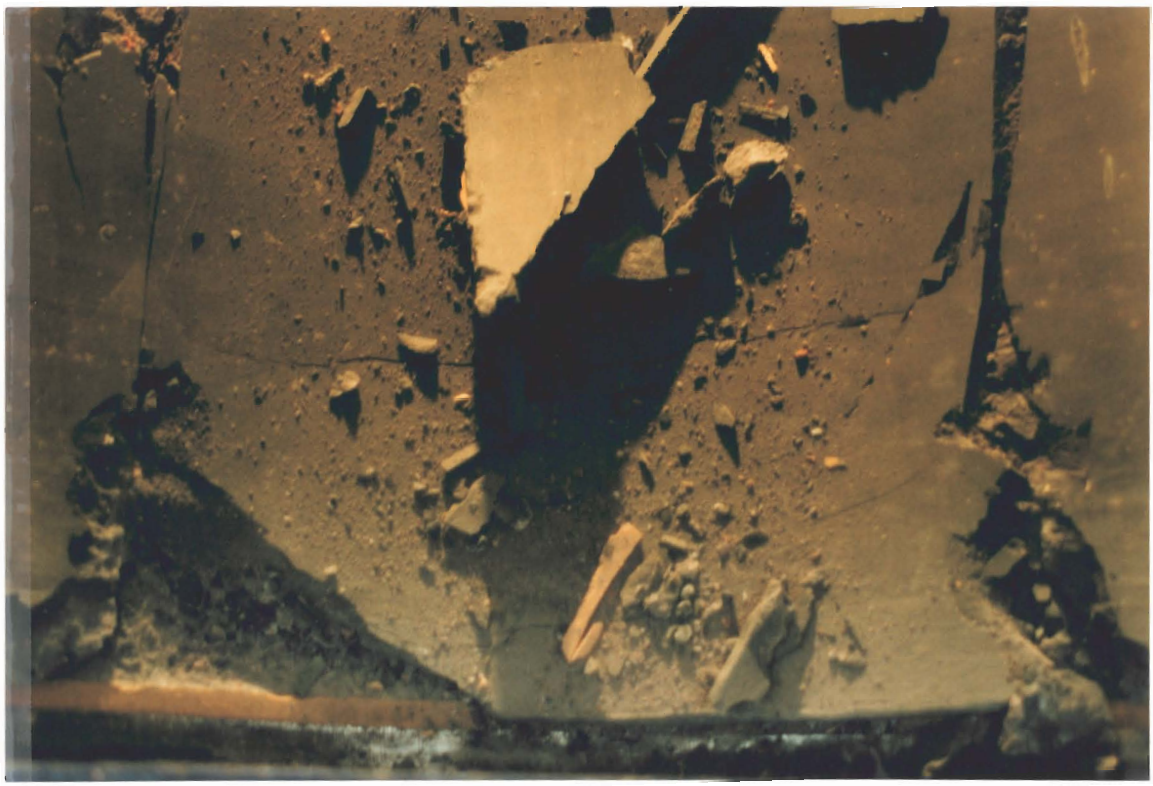

Plate D6 Pipe 7: Standard pipe (1.0° deflection)

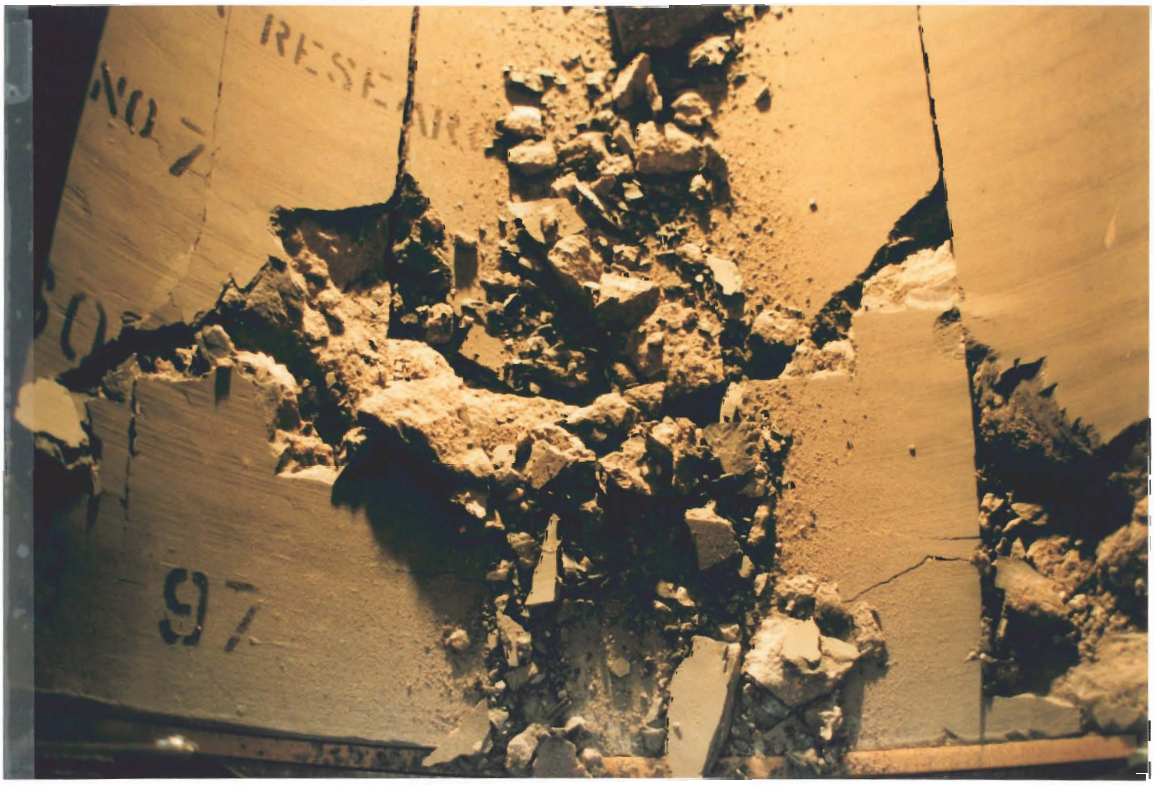

Plate D7 Pipe 9: Standard pipe with joint reinforcement (1.0° deflection)

Plate D8 Pipe 10: Standard pipe with joint reinforcement (1.0° deflection)

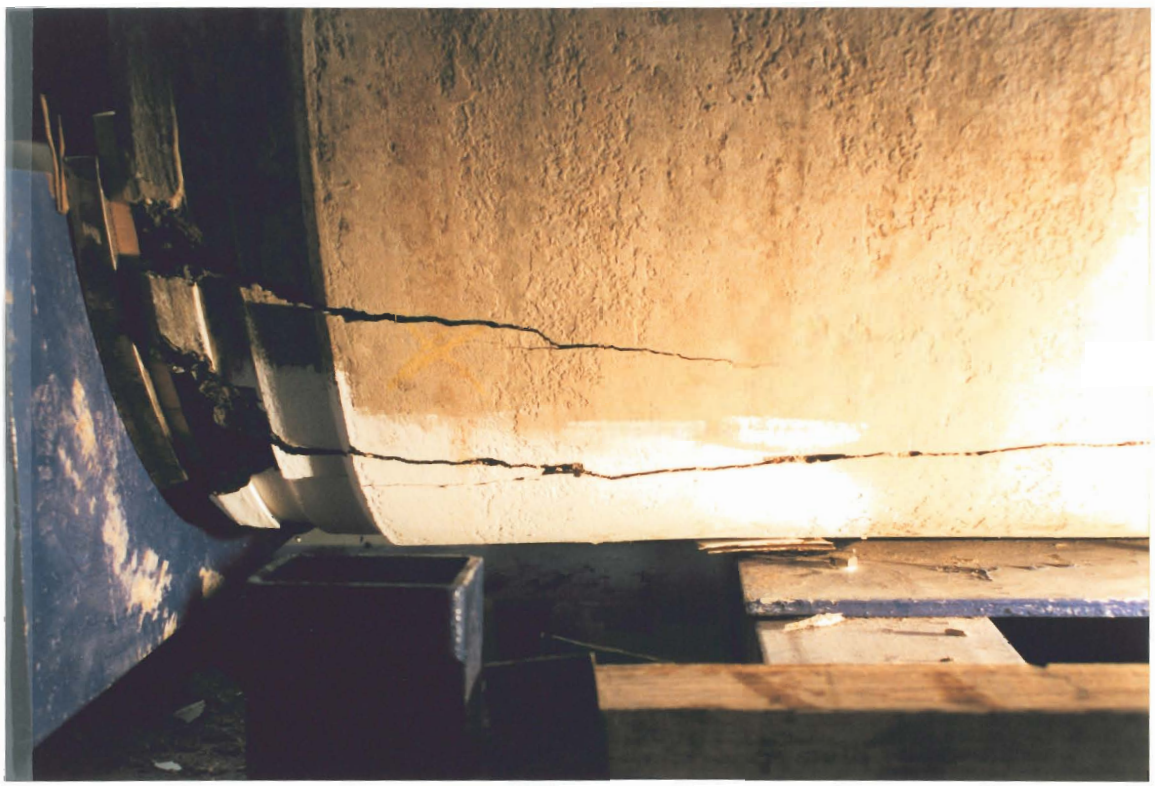

Plate D9 Pipe 11: Standard pipe with 3° chamfer and joint reinf't (1.0° deflection)

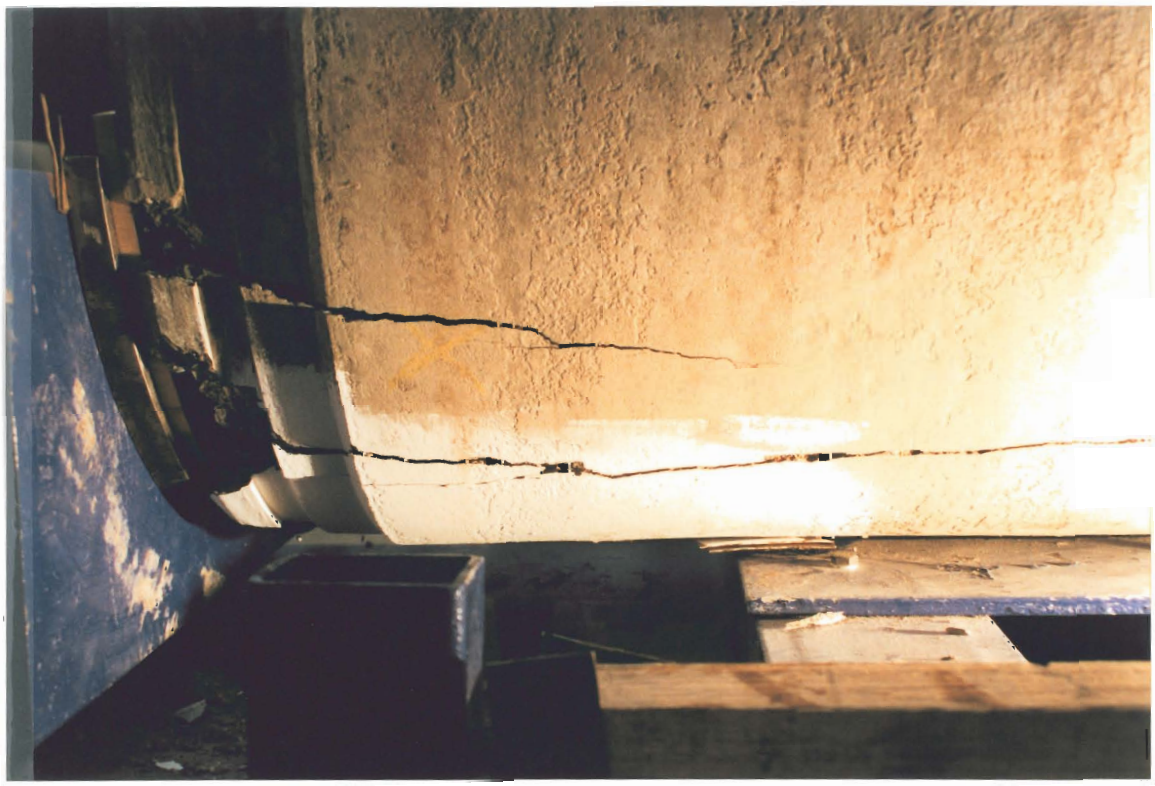

Plate D9 Pipe 11: Standard pipe with 3" chamfer and joint reinf (1.0° deflection)

Plate D10 Pipe 12: Standard pipe with 3° chamfer and joint reinf't (1.0° deflection)

Plate **D1**1 Pipe 1: Standard pipe (0.5° deflection)

Plate D12 Pipe 2: Standard pipe with 2° chamfer (0.5° deflection)

Plate D1 3 Pipe 3: Pipe with joint reinforcement (0.5° deflection)

Plate D14 Pipe 4: Standard pipe with 3° chamfer and joint reinft (0.5° deflection)

Plate D15 Pipe 5: Standard pipe with 3° chamfer and joint reinf't (0.5° deflection)

Plate D16 Pipe 6: Standard pipe (1.0° deflection)

Plate D17 Pipe 7: Standard pipe (1.0° deflection)

Plate D18 Pipe 8: Standard pipe with 2° chamfer (1.0° deflection)

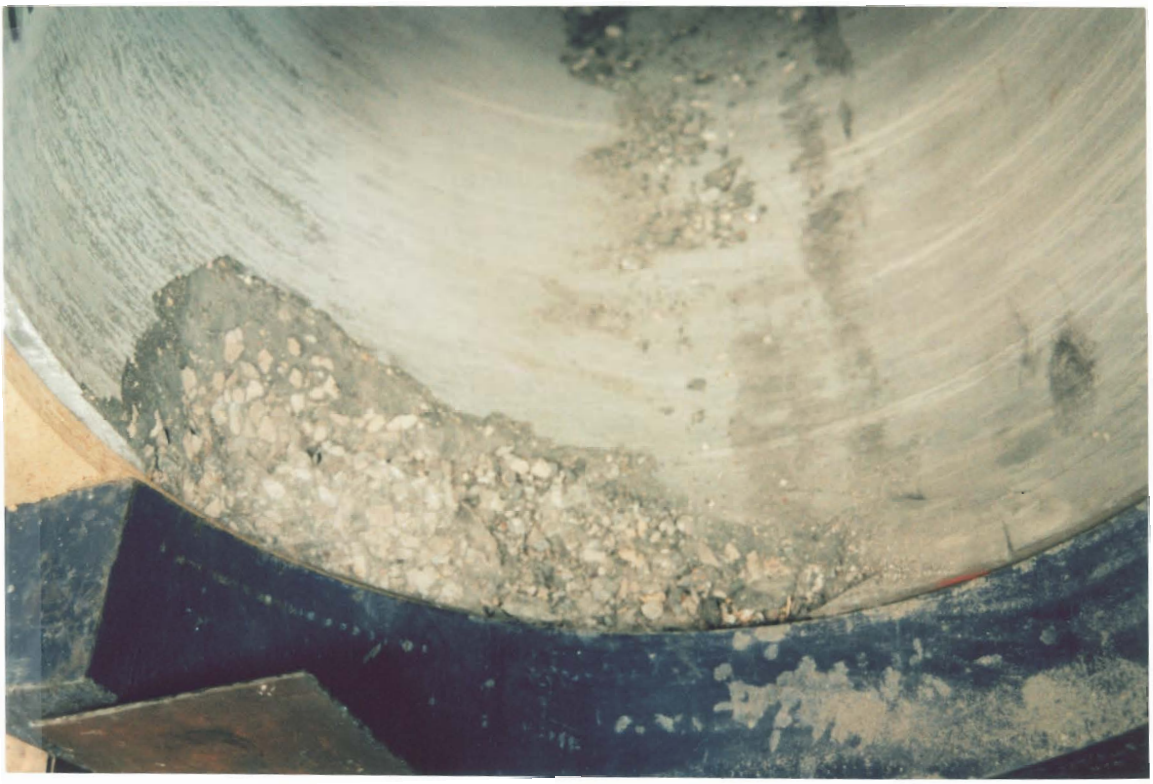

Plate D19 Pipe 9: Standard pipe with joint reinforcement (1.0° deflection)

Plate D20 Pipe 10: Standard pipe with joint reinforcement (1.0° deflection)

Plate D21 Pipe 11: Standard pipe with 3° chamfer and joint reinf't (1.0° deflection)

Plate D22 Pipe 12: Standard pipe with 3$^{@}$ chamfer and joint reinf't (1.0^{v} deflection)

Plate D23 Pipe 13: Standard pipe unreinforced (1.0° deflection)

Plate D24 Pipe 14: Standard pipe unreinforced with 2° chamfer (1.0° deflection)

Plate D24 Pipe 14: Standard pipe unreinforced with 2° chamfer (1.0° deflection)

Plate D25 Pipe 1: Standard pipe (0.5° deflection)

Plate D26 Pipe 2: Standard pipe (0.5° deflection)

Plate D27 Pipe 3: Standard pipe with 1 presressed steel band (0.5° deflection)

Plate D28 Pipe 4: Standard pipe with 1 presressed steel band (0.5° deflection)

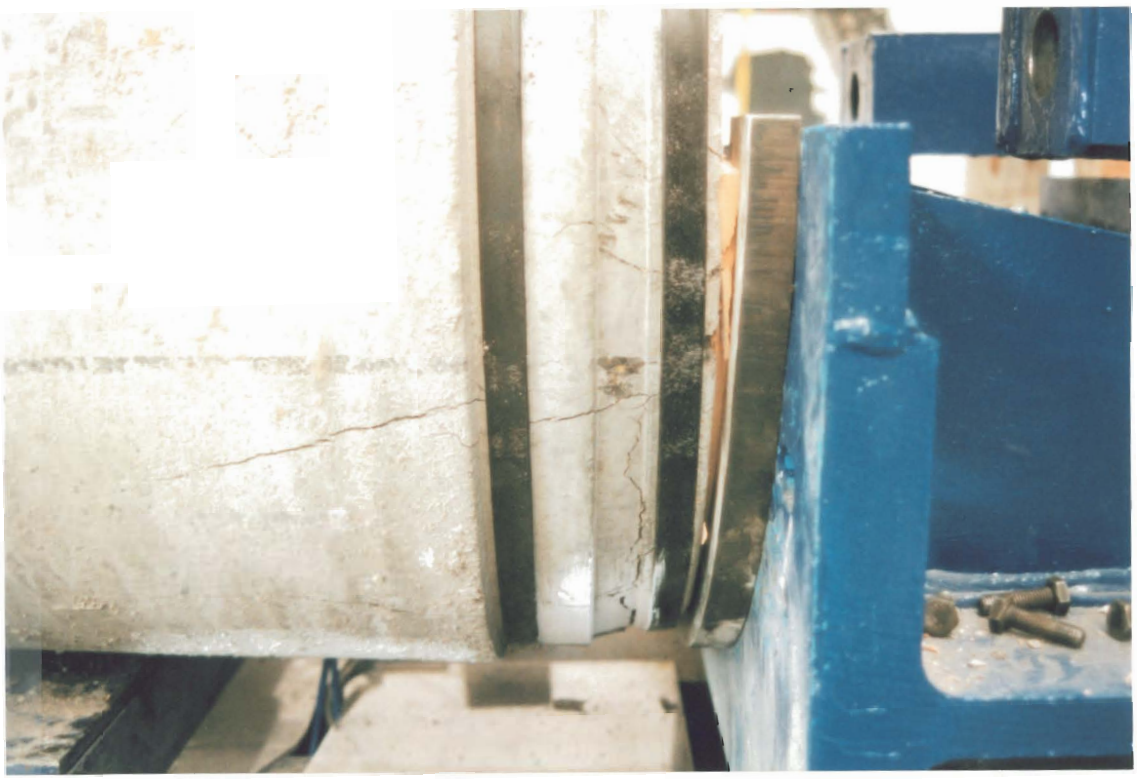

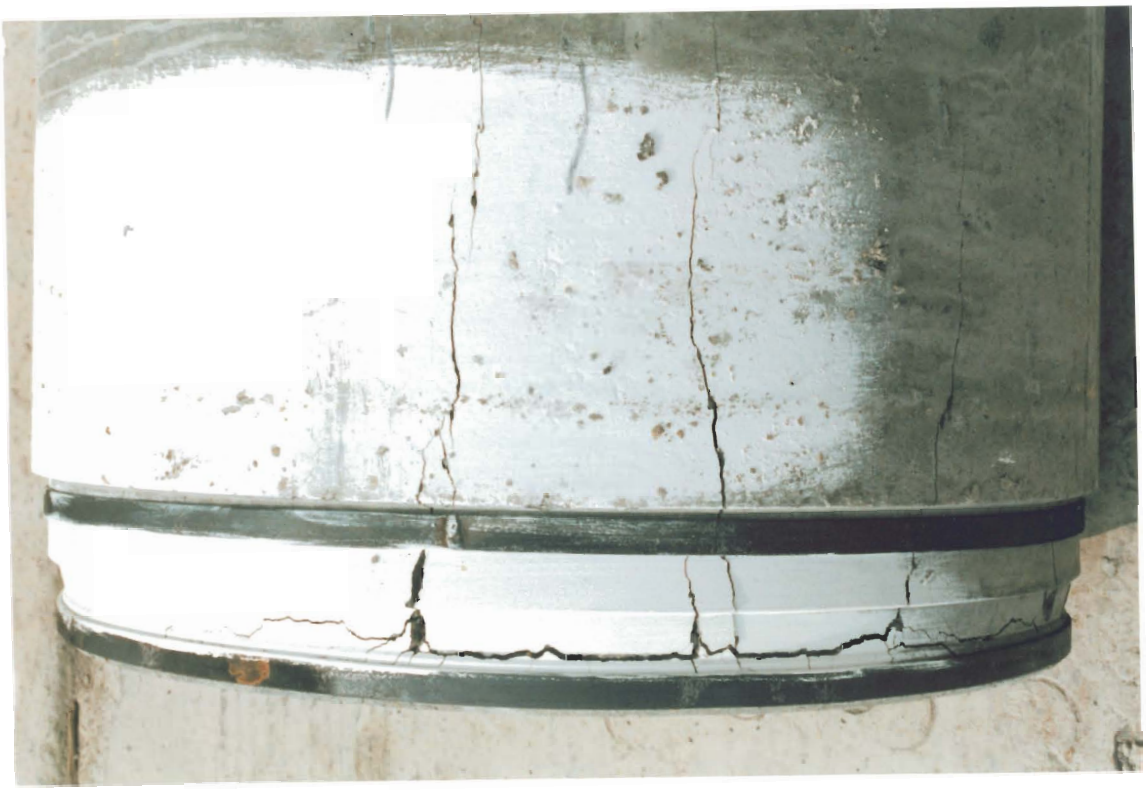

Plate D29 Pipe 5: Standard pipe with 2 presressed steel bands (0.5° deflection)

Plate D30 Pipe 6: Standard pipe with 2 presressed steel bands (0.5° deflection)

Plate D31 Pipe 7: Standard pipe (1.0° deflection)

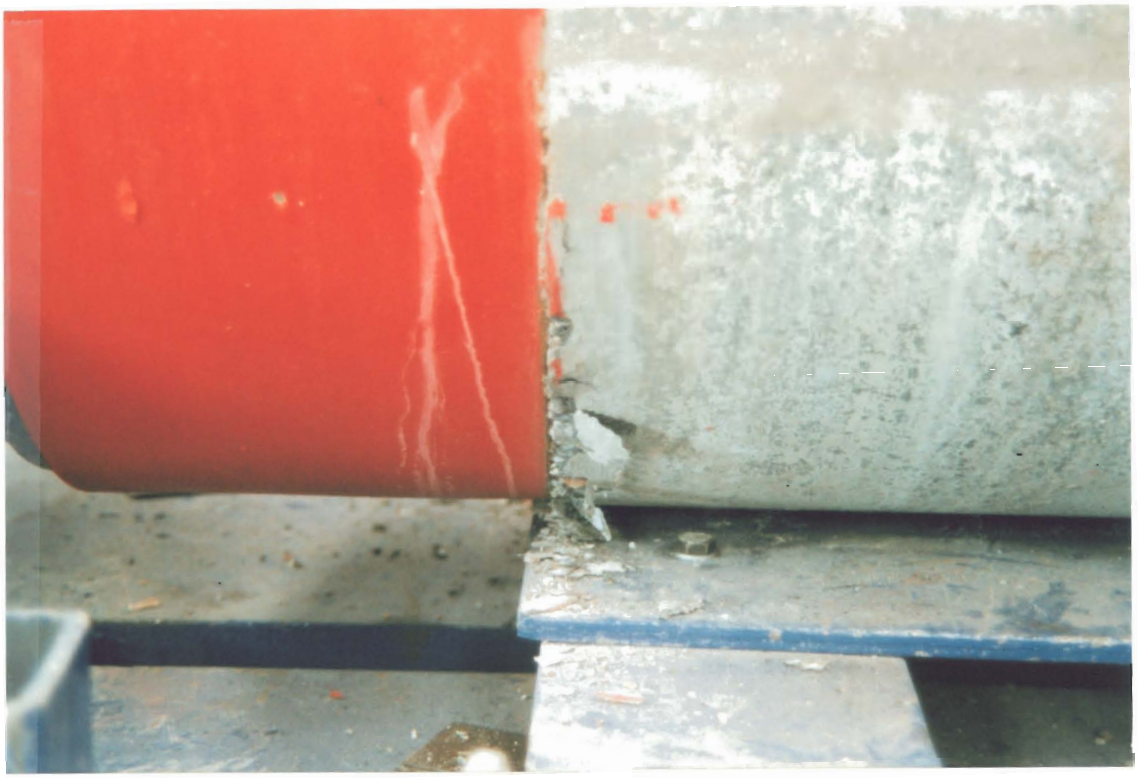

Plate D3.2 Pipe 8: Standard pipe (1.0° deflection)

Plate D33 Pipe 9: Standard pipe with 1 prestressed steel band (1.0° deflection)

Plate D34 Pipe 10: Standard pipe with 1 pressed steel band (1.0° deflection)

Plate D35 Pipe 11: Standard pipe with 1 presressed steel band (1.0° deflection)

Plate D36 Pipe 12: Standard pipe with 2 prestressed steel bands (1.0° deflection)

APPENDIX E

Summary of tests carried out on GRP pipes supplied by Johnstons

Towards the end of the testing programme Johnstons approached the University of Oxford, via the PJA expressing an interest in testing two GRP microtunnelling pipes. These pipes were outside the initial scope of the research programme for two reasons. Firstly no modifications had been incorporated to the spigot end and secondly the material the pipes were made of was significantly different to the concrete used in the manufacture of the pipes already tested. Subsequently only a description of the failure mechanism and failure load are presented here. No comparisons are made with the concrete pipes previously tested.

Both GRP pipes supplied were 1.2m long, in order to fit the test rig, however, this length was cut from a pipe that was considerably longer. The wall thickness of the barrel of the pipe was 50mm, reducing to a minimum dimension of approximately 34mm at the spigot end. Both pipes were tested in a similar manner as the previous pipes tested. Both pipes were tested at a deflection angle of 1.0^{o}.

The following is a description of the failure mechanism observed for each pipe. An ultimate failure load is also presented.

Pipe 1 (tested at 1.0^{o})
Ultimate failure load 2192 kN

An "explosive" failure of the pipe occurred. At failure segments of pipe from the spigot end became detached from the loaded part of the spigot end. The only part of the pipe to fail was the spigot end. No other areas of distress were observed. Before failure occurred the fibres within the pipe made a "cracking" noise. Shortly afterwards failure of the pipe occurred. This cracking gave a good indication of when failure was going to occur.

During load application no spalling or cracking was observed.

Pipe 2 (tested at 1.0^{o})
Ultimate failure load 2208 kN

The mode of failure was similar to that described for pipe 1